Spring 5-2015

The Development and Evaluation of a Method for Understanding the Impact of Transmission Loss On the Overall Noise Attenuation of Finite Barriers

Ashwin Arvind Upasani
Rose-Hulman Institute of Technology

THE DEVELOPMENT AND EVALUATION OF A METHOD FOR UNDERSTANDING THE IMPACT OF TRANSMISSION LOSS ON THE OVERALL NOISE ATTENUATION OF FINITE BARRIERS

A Thesis

Submitted to the Faculty

of

Rose-Hulman Institute of Technology

by

Ashwin Arvind Upasani

In Partial Fulfillment of the Requirements for the Degree

of

Master of Science in Mechanical Engineering

May 2015

ROSE-HULMAN INSTITUTE OF TECHNOLOGY

Final Examination Report

Ashwin Arvind Upasani — Name

Mechanical Engineering — Graduate Major

Thesis Title **The Development and Evaluation of a Method for Understanding the Impact of Transmission Loss on the Overall Noise Attenuation of Finite Barriers**

DATE OF EXAM: **April 22, 2015**

EXAMINATION COMMITTEE:

	Thesis Advisory Committee	Department
Thesis Advisor:	**Darrell Gibson**	**ME**
	Jerry Fine	**ME**
	Eva Andrijcic	**EMGT**

PASSED X **FAILED** _____

ABSTRACT

Upasani, Ashwin Arvind

M.S.M.E

Rose-Hulman Institute of Technology

May 2015

The Development and Evaluation of a Method for Understanding the Impact of Transmission Loss on the Overall Noise Attenuation of Finite Barriers

Thesis Advisor: Dr. Darrell Gibson

The purpose of this study is to evaluate the impact of transmission loss on the overall noise reduction obtained from finite barriers. The noise attenuation ability of barriers is understood to be a consequence of sound waves diffracting around their edges. Although the presence of transmission loss is acknowledged, its significance in affecting noise attenuation is usually not considered a priority in barrier design. This study incorporates the Fresnel Number concept for predicting theoretical insertion loss of a finite barrier and compares these predictions to experimental observations. The experiments performed in this study offer a method to isolate the transmission loss component from diffraction based noise attenuation. This isolation allows the comparison of these two factors in the overall barrier performance. The influence of transmission loss is found to be significant and the findings encourage its consideration in designing solutions to modern noise control challenges.

DEDICATION

In Memory of Abhishek Bangale

An Optimist, A True Friend, An Undaunted Fighter

Always Present, in the Good Times and the Bad

ACKNOWLEDGEMENTS

I would like to express my sincere gratitude to Dr. Darrell Gibson for his assistance and guidance during this study. I would also like to express my gratefulness to Dr. Eva Andrijcic and Dr. Jerry Fine for their continuous support and invaluable advice during my research work. As my advisory committee, their encouragement has been fundamental to my academic journey at Rose-Hulman Institute of Technology.

I would like to extend a special thank you to Dr. Edward Wheeler for providing access to his lab, which made the experimental investigations in this study possible.

I would also like to convey my gratefulness to the Learning Center for proofreading my drafts and offering crucial suggestions. My sincere appreciation also goes to the Library staff, especially Bernadette Ewen and Amy Harshbarger for their indispensible efforts in providing research materials that were essential for this study. A special thank you also to the Graduate Office for providing the financial opportunities that encourage and support graduate research.

My most sincere appreciation goes to my parents and my family. Their encouragement and hard work has been vital in providing an environment full of opportunities and possibilities for success.

Last but not the least, I would like to express my deepest gratitude to Isabella Magni for her assistance with the experiments and draft corrections. Her encouragement, kindness, and unconditional support have been fundamental to this journey for which I will be forever grateful.

TABLE OF CONTENTS

LIST OF FIGURES

LIST OF TABLES

LIST OF ABBREVIATIONS

OSHA	The Occupational Safety and Health Administration
FAA	The Federal Aviation Association
HUD	The Department of Housing and Urban Development
IL	Insertion Loss
TL	Transmission Loss
SPL	Sound Pressure Level
SLM	Sound Level Meter
NR	Noise Reduction
rms	Root Mean Squared

LIST OF SYMBOLS

English Symbols

TL	Transmission Loss
IL_d	Diffraction based Insertion Loss
dB	Decibels
Hz	Hertz
N	Fresnel Number
L_p	Sound Pressure Level in decibels
f	Sound Frequency
f_c	Critical Frequency of Transmission Loss
W	Power of Sound Source
Q	Directivity Factor
t	Thickness of barrier
c	Speed of sound in medium

Greek Symbols

ρ	Density of Medium
τ	Transmission Coefficient
δ	Path Difference
λ	Wavelength
θ_i	Angle of incidence

GLOSSARY

Insertion Loss: The reduction in the SPL at a particular location due to the insertion of an object between the source and the receiver location.

Transmission Loss: The measure of the sound insulation provided by a partition of a given material and size as a result of a loss in sound intensity from sound waves traveling through the partition.

Diffraction: The bending of sound waves around an object that obstructs its original direction of travel.

Noise Attenuation: The reduction in the SPL at a particular location.

Finite Barrier: An object placed between the sound source and a receiver location that results in the diffraction of sound waves over its top edge and around its side edges for the purpose of noise attenuation.

Decibel: A logarithmic unit used to express sound pressure levels

Reverberation: The reflections of sound waves in an enclosed space that creates a sound pressure level build-up.

Chapter I: INTRODUCTION

In the past few decades, barriers have been extensively used for noise reduction purposes in indoor and outdoor environments. As environmental awareness has increased and the effects of technology and human activities on health and environment are being better understood, the issue of noise pollution has come to the forefront along with all the other sources of pollution. In the United States of America, The Occupational Safety and Health Administration (OSHA) undertakes the task of introducing rules and regulations, and enforcing appropriate standards to maintain healthy and safe conditions for working individuals. OSHA is part of the Department of Labor and was created by Congress after passing the Occupational Safety and Health Act in 1970 [1]. OSHA has improved the awareness of the negative impacts of noise and strived to create healthy working environments in various industries. Over the years, OSHA's industrial regulations have translated into increased awareness about the consequences of noise pollution in non-industrial sections of society. Various organizations such as the Federal Aviation Association (FAA), Department of Housing and Urban Development (HUD), etc. have developed their own noise standards to address noise issues related to activities that fall under their respective organizations [2]. Consequently, there is an increasing demand for engineers to develop efficient, effective, and economic solutions for noise reduction.

Scientific research and experience has shown that loud noise (approximately above 85 dB) can cause various degrees of temporary or permanent hearing loss depending on the duration of exposure [2]. Other consequences of loud noise include headaches, dizziness, high levels of

stress, loss of sleep, disturbances in wildlife habitat, etc. Noise reduction solutions are obviously required to prevent such problems, however, there is also a considerable increase in demand for providing solutions in noise quality, improving office atmosphere to enhance productivity, and increasing residential noise insulation for comfort and privacy. Various noise control methods are available, which include the use of noise barriers, sound absorbing materials, acoustical enclosures, vibration control at noise source, and vibration damping. Barriers are extensively used to provide cheap and effective solutions to noise control problems and this noise control method is further investigated in this thesis.

The noise reduction ability of barriers is a direct result of the diffraction of sounds waves as they attempt to travel past the barrier. Diffraction of sound waves can provide considerable noise attenuation at higher sound frequencies but can also be significant for lower frequencies. The noise reduction provided by placing a barrier between the source and the receiver is called the Insertion Loss (IL). Maekawa, and Moreland and Musa have established theoretical expressions for IL based on diffraction theory [3,4]. However, in practice the IL is usually lower than the expected theoretical value because of the transmission of sound waves through the barrier. The Transmission Loss (TL) is usually ignored by choosing high-density barrier materials or thick barriers in order to reduce the transmission of sound through barriers. Although TL may not have a huge impact on overall IL for semi-infinite barriers since the sound waves can only bend around the top edge of the barrier, it could prove to be considerable in the case of finite barriers. Sound waves have the opportunity to bend around the top edge as well as the side edges while using finite barriers, and the theoretical IL offered by such barriers might not be as significant as semi-infinite barriers. Therefore, it would be advisable to consider the impact of TL on the overall IL while designing such barriers. Furthermore, from a business

perspective, it would be valuable for the barrier manufacturer to understand the impact of TL on overall noise attenuation in order to optimize the design of the barrier by maximizing noise reduction and using the least amount of barrier material.

This thesis examines the impact of TL on the overall IL of finite barriers by using a method to isolate the effect of sound transmission from the diffraction of sound waves. The motivation for this study was derived from the study of finite barrier performance in noise attenuation by Iyer [5]. In this study, the author attributes the departure of experimental IL readings from the theoretical values to reflections off the walls of the enclosed space. Another study on the performance of finite barriers by the author and Li showed some evidence that the TL could have a considerable impact on the overall performance of finite barriers [6]. This thesis aims at investigating the issue further. The experiments in this study were performed on plywood barriers, as it is a fairly inexpensive material and it can offer significant noise reduction. The experiments were performed at various sound frequencies because barrier performance is frequency dependent.

Chapter II: BACKGROUND

There are various factors that affect the overall performance of barriers. Among these factors are the shape and orientation of barriers. Numerous creative shapes and orientations have been investigated for achieving desired noise attenuation. Some of these include case studies where natural objects such as soil, vegetation, etc. were considered to be used as barriers. Figure 2.1 shows an example of a noise barrier made from mulch to reduce highway noise [7]. There are numerous advantages and disadvantages to various forms of barriers that are case dependent and investigating this wide variety is not within the scope of this thesis. This study primarily focuses on standard, vertically oriented, and flat-shaped barriers. The investigations and discussion presented by the author are only applicable to this form of barriers.

Figure 2.1. The Great Wall of Mulch is an example of a vegetative noise barrier [7]

2.1 Types of Barriers

2.1.1 Semi-Infinite Barriers

Discussions of sound diffraction theory describe a semi-infinite barrier as an object whose length is large enough such that it can be considered to be infinitely long for a given sound source. For example, a highway barrier would be considered to be infinite from the point of view of a car. The fundamental characteristic of a semi-infinite barrier is that its long length does not allow sound waves from the source to bend around the side edges of the barrier. Therefore, the noise attenuation achieved at the receiver using such barriers is a result of the bending of sound waves over the top of the barrier.

2.1.2 Finite Barriers

Finite barriers, as the name suggests, are the opposite of semi-infinite barriers in the characteristics of their length. The length of such barriers is short enough to allow the sound waves from the source to bend around the side-edges of the barrier. The difference in the physical setup has a direct impact on the noise attenuation provided by the barrier due to the additional diffraction paths available to the travelling sound waves. An example of this type of barrier could be a panel placed next to stationary manufacturing equipment in a factory to reduce noise levels experienced by an office space. The experiments and investigations in this thesis will focus on the noise attenuation characteristics of such barriers.

2.1.3 Reflective Barriers

Reflective barriers are generally made from common construction materials such as concrete, lightweight concrete, wood, metal sheeting, plastics, glass, etc. Among these, concrete

and wood are the most frequently used materials. Various types of wood with a range of densities can be used as barriers and the thickness of wooden panels can be easily customized. Concrete barriers usually consist of stacked panels, which have a thickness of 90 to 200 mm and a surface density of 200 to 400 kg/m^2 [8]. Lightweight concrete or some fibrous cement are also used for making reflective barriers. However, these materials offer lower densities, which affect TL, but this factor is usually not a priority as mentioned previously.

Thin metal sheets manufactured from steel and aluminum with thicknesses ranging from 1 to 2 mm also provide noise attenuation solutions [8]. One of the challenges of using metal barriers is to achieve appropriate TL by managing barrier thickness. Achieving high TL is particularly important at lower frequencies.

Glass and plastic barriers can also prove to be effective noise control solutions. The reflective nature of plastic barriers depends on their surface density and most of them tend to be absorptive rather than reflective. The use of reflective glass barriers has been increasing in recent times. Acrylic or a polycarbonate resin type of glass is used to manufacture barriers with thicknesses ranging from 5 to 8 mm. Glass barriers made from polymethylmethacrylate have thicknesses ranging from 15 to 20 mm. The average surface density of such barriers is 10 to 20 kg/m^2 [8]. A very important advantage of using glass barriers is the improved visibility due to its transparent nature. For example, glass barriers used to reduce transportation noise from sources such as highway traffic and railways can offer drivers and passengers landscape visibility. The subjects in the noise shadow zone are also offered increased visibility, which could be beneficial if the barrier is providing noise attenuation to a residential area. A major disadvantage of such barriers is the reflection off of the glass, which is an important design consideration. Another

problem for these barriers is the need for frequent cleaning of glass. However, this problem can be overcome by careful design and inclining the barrier construction.

2.1.4 Absorptive Barriers

Absorptive noise barriers are a considerably recent solution to noise attenuation issues and are not used as frequently as reflective barriers. The most common absorptive barrier materials are various composites, ceramics, sintered metals, cement-bonded wood-wool or wood-chips, aerated concrete, etc. They are generally divided into two broad categories: Systems with Cavities Incorporating Absorbing Materials and Systems with Panels of Open Textured Porous Materials [8].

A common example of systems with cavities is perforated metal boxes containing fibrous materials. Another example is a construction of cement or baked clay blocks with internal cavities. In the latter, the source side of the barrier contains holes or slots and sound is absorbed at the resonant frequencies of the cavities. Using fibrous or foam filters can extend the range of absorbed frequencies [8].

The materials commonly used in the systems with panels include porous cement and concrete, wood chips in a cement matrix and small particles in an epoxy matrix. Particles of hard porcelain are used to make ceramic sound absorbers, which are shaped into porous boards with thicknesses ranging from 10 to 50 mm. This material is extremely resistant to chemicals and high temperatures. However, this material does not have high structural strength to withstand strong impact forces. Common absorptive material used for highway and railway noise attenuation is made from wood fibers bonded with cement that is 50 to 100 mm thick and backed with a solid concrete panel [8]. Absorption within the materials is achieved by inertial and frictional losses.

These barriers usually include a hard backing to prevent transmission of sound through the barrier. For barriers mounted directly on a backing, 50 to 100 mm thickness panels provide good absorption characteristics at low frequencies. The front faces of panels are also usually curved rather than flat. Air gaps introduced between the panel and the backing can further improve noise attenuation from such barriers and can help reduce the thickness of barrier panels. Such creative design techniques can be used to reduce material costs and improve the mobility of these kinds of barriers.

2.2 Factors Affecting Barrier Performance:

2.2.1 Barrier Height and the Proximity of Source and Receiver from the Barrier

The height of the barrier and its distance from the source and receiver play a very important role in the overall noise attenuation offered by the barrier. These factors are used to identify the Fresnel number of the system, which is an essential factor in determining the theoretical IL provided by barriers using diffraction theory. This phenomenon will be described in more detail in the next chapter.

Different applications have different standards for the height and barrier-source distance based on the characteristics of the noise source. For example, railway barriers are usually shorter (1.5 to 2 m) compared to highway barriers (6 to 7 m) because the proximity of the source in railway applications is able to offer considerable noise attenuation for short barriers [8].

2.2.2 Sound Absorbing Material

Using sound absorbing material on the source side of a barrier can lead to improved barrier performance in most cases. The improvement offered by the absorbing material depends

on various factors such as type of absorbing material, density of the material, frequency of sound, angle between the absorbing barrier surface and the ray from the source to the top of the barrier, etc. The increase in the IL is more significant if the source or the receiver is close to the barrier [8]. The fundamental characteristics of absorptive materials that improve barrier performance are the ability to reduce the diffraction of sound waves into the shadow zone[1] and reduce the reflections between the source and the barrier, which prevents multiple incident sound waves and diffractions. These characteristics can be visually observed in Figure 2.2.

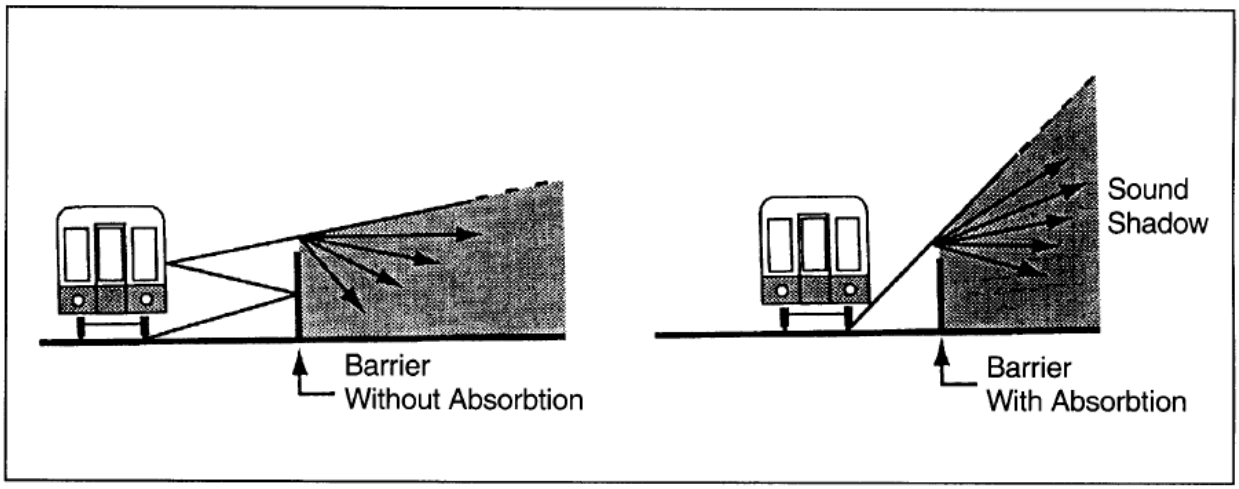

Figure 2.2. The effect of barriers with sound absorbing material on the diffraction of sound [8]

2.2.3 Surface of the Source

Reflection of sound waves is dependent on the sound source as well as the barrier. Bulky or high-density sound sources can lead to multiple reflections and negatively impact the performance of barriers. The impact of reflections is particularly worse if the noise source is close to the barrier. Figure 2.3 illustrates how reflections off a sound source affect barrier

[1] Noise attenuation on the receiver side of a sound barrier can be thought of creating an acoustic shadow similar to shadows created by walls or similar opaque objects. The shadow zone is the area on the receiver side in which the noise attenuation capabilities of the barrier can be observed. The noise attenuation in the shadow zone is frequency dependent [9].

performance and this effect is seen to be particularly worse because the sound source is higher than the barrier [8].

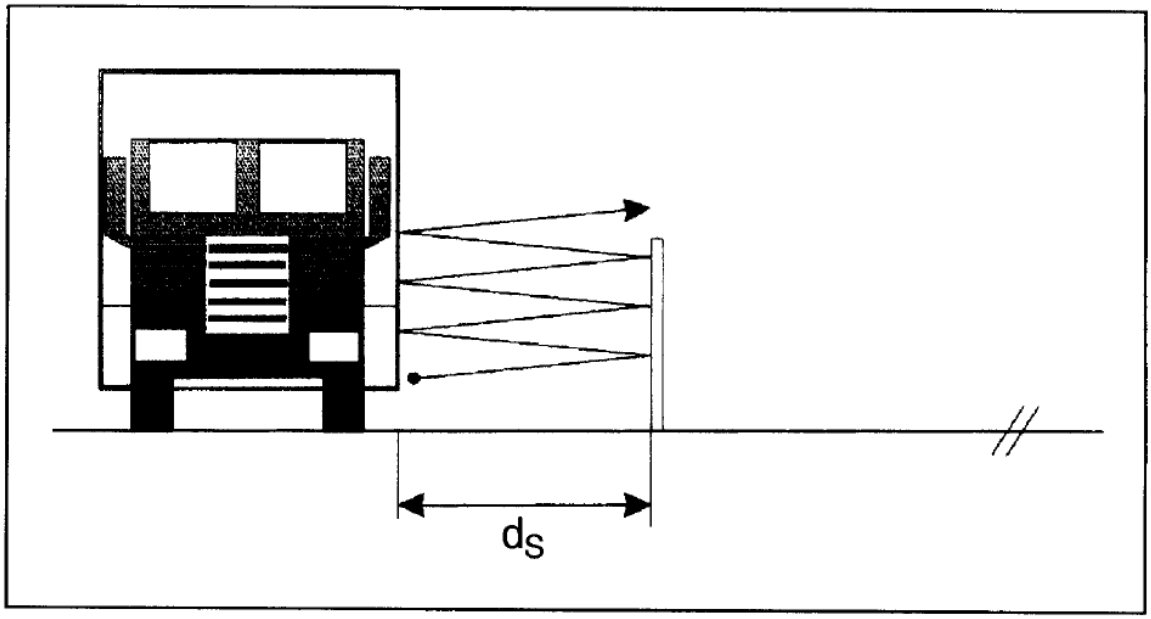

Figure 2.3. The effect of reflections on the performance of sound barriers [8]

2.2.4 Frequency of Sound and its Effect on Diffraction

As discussed previously, numerous factors affect the performance of barriers, but the fundamental feature that allows the use of barriers for noise attenuation is the wave nature of sound. The wave nature of sound allows it to be reflected, absorbed, transmitted, and diffracted, and all of these phenomena affect the overall performance of a noise barrier. However, diffraction, which is the ability of sound waves to bend around the top and side edges of the barrier, is the most important physical phenomenon in the noise reduction process. It is important to consider the effects of frequency (or wavelength) on diffraction because it results from the wave nature of sound. It is known that higher sound frequencies diffract less and they can be guided away from the receiver. In contrast, lower frequencies diffract more which makes it

difficult to achieve high IL values for these frequencies. Figure 2.4 illustrates the difference in the diffraction properties of sound waves for different frequencies [10].

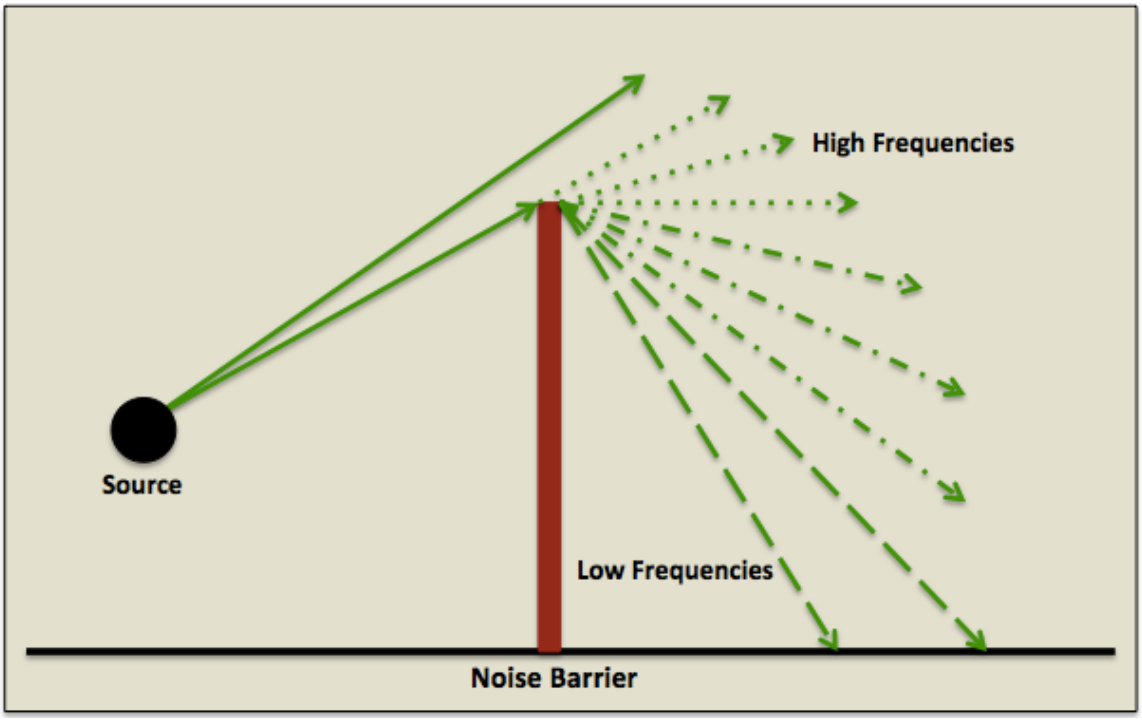

Figure 2.4. Frequency dependent barrier diffraction [10]

2.2.5 Transmission Loss

The typical interpretation of IL from barriers accounts for the noise attenuation due to diffraction of sound waves and considers the TL to be negligible. As shown in Figure 2.5, this is not exactly accurate because the transmission of sound waves through the barrier has an impact on the sound level at the receiver (overall IL due to the barrier). Typically, barriers are made from high-density construction materials and in such cases the TL may be negligible in the overall performance of the barrier. However, in an indoor environment, the use of bulky, high-density construction material could be inconvenient. In such cases, it could be important to understand the impact of TL on the overall IL, as it would provide useful guidelines in the design

of cheap and effective barriers. It is also challenging to measure and isolate the effect of TL on finite barriers due to interference from diffracting sound waves. This is because the standard methods of measuring TL do not allow diffracting sound to interfere with the Sound Pressure Level (SPL) measurements.

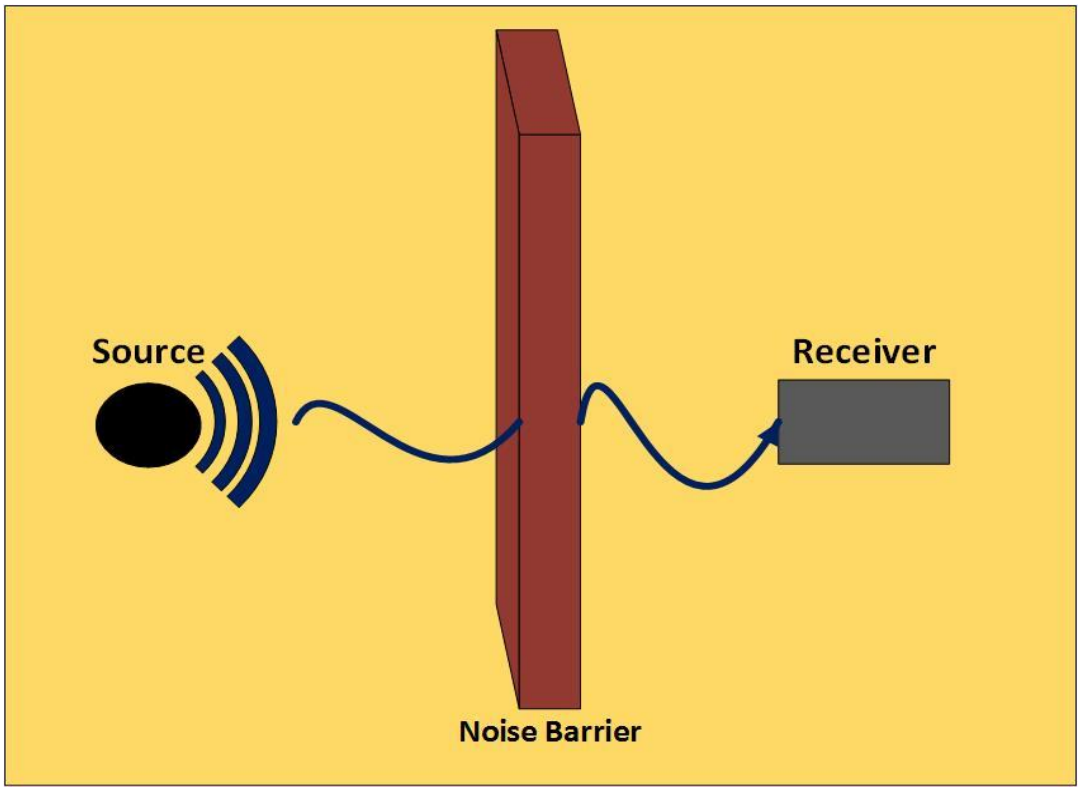

Figure 2.5. The transmission of sound waves through the barrier affects the overall IL

This thesis focuses on determining the impact of TL on the overall performance of barriers by using a method that will be discussed in the following chapters. It takes into account that the performance of barriers is frequency dependent and evaluates the impact of TL at various frequencies to better understand their relationship.

Chapter III: LITERATURE REVIEW

3.1 Sound Pressure Level (SPL)

The level of sound heard by the human ear depends on the acoustic pressure it experiences. The range of acoustic pressure that is of interest in the area of noise control varies between 10^{-9} psi to approximately 15 psi (1 atm.) [2]. The human ear is most sensitive to sound levels that lie within this pressure range. Since the range of interest is extremely wide, sound pressure levels are usually measured by using the unit of decibels (dB). A decibel is a dimensionless logarithmic unit that compares measured sound pressures to a reference pressure, thereby reducing this wide range of interest into a more manageable and comparable range of values. Acoustical engineers have universally adopted the dB unit and it is a widely accepted standard in the area of acoustical studies. The SPL in dB, which is symbolically represented as L_p is defined as

$$L_p = 10\ log_{10}\left(\frac{p^2}{p_{re}^2}\right) \qquad dB \tag{3.1}$$

where,

p = root-mean-square (rms) sound pressure in Pa

p_{re} = international reference pressure of 2.0×10^{-5} Pa

Equation 3.1 can be simplified and expressed in a much more useful form as follows:

$$L_p = 20\ log_{10}\ (p) + 94 \qquad dB \tag{3.2}$$

The international reference pressure was chosen to have the given value because it has been found to be the average threshold of hearing for young adults while listening to a pure frequency tone of 1000 Hz [2]. In general, the human ear is not very sensitive in detecting a 2 to 3 dB change in SPL. However, the ear can sense a difference in 10 to 20 dB and higher changes such as 35 to 40 dB are experienced as dramatic changes. Figure 3.1 is a good reference for understanding the acoustic pressures and their corresponding decibel values for some typical sounds experienced by humans.

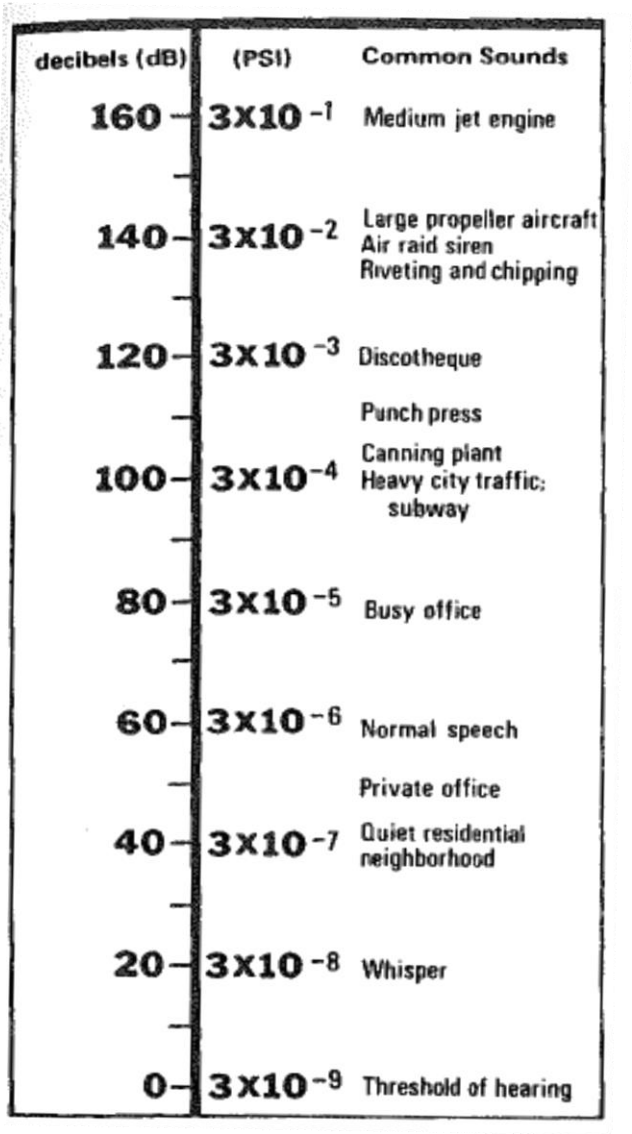

Figure 3.1. Examples of everyday sounds compared using the dB scale and psi scale of SPL [2]

3.2 Diffraction Theory

When sound waves arrive upon an obstacle in the form of a barrier, some of them are reflected back while some of them are transmitted. Some of the waves may be absorbed if the barrier material offers any absorptive properties. The remaining sound waves bend around the obstacle and this property is known as diffraction. Diffraction of sound casts an acoustical shadow where some level of noise attenuation is achieved due to the inserted obstacle.

3.2.1 Noise Attenuation from Semi-Infinite Barriers

The studies performed by Maekawa, Kurze and Anderson, et al. has led to a considerable amount of literature on the effect of semi-infinite barriers on noise attenuation based on diffraction theory [3,9]. In the case of semi-infinite barriers, sound waves can only bend over the top of the barrier. Therefore, the most significant factors affecting the overall noise attenuation are the height of the barrier, and the distance of the source and the receiver from the barrier. Figure 3.2 shows the important parameters affecting semi-infinite barrier performance. Based on diffraction theory, the noise attenuation can be given as:

$$IL_d = 20\ log_{10}\left(\frac{\sqrt{2\pi N}}{\tanh\sqrt{2\pi N}}\right) + 5 \qquad (N > 0) \qquad dB \qquad (3.3)$$

where,

$$N = Fresnel\ Number = \frac{2\delta}{\lambda} \qquad unitless$$

The factor δ is defined as the difference between the diffracted path due to the insertion of the barrier and the direct path in the absence of the barrier. For the parameters shown in Figure 3.2, the path difference can be mathematically expressed as:

$$\delta = \sqrt{S^2 + h^2} - S + \sqrt{R^2 + h^2} - R \qquad m \tag{3.4}$$

where,

S = distance from the source to the barrier along the line of sight (m)

R = distance from the receiver to the barrier along the line of sight (m)

h = effective barrier height (projected height of the barrier along the line of sight)

Equation 3.4 can be simplified and expressed as:

$$\delta = A + B - d \qquad m \tag{3.5}$$

where,

$A = \sqrt{S^2 + h^2}$ m

$B = \sqrt{R^2 + h^2}$ m

d = S + R m

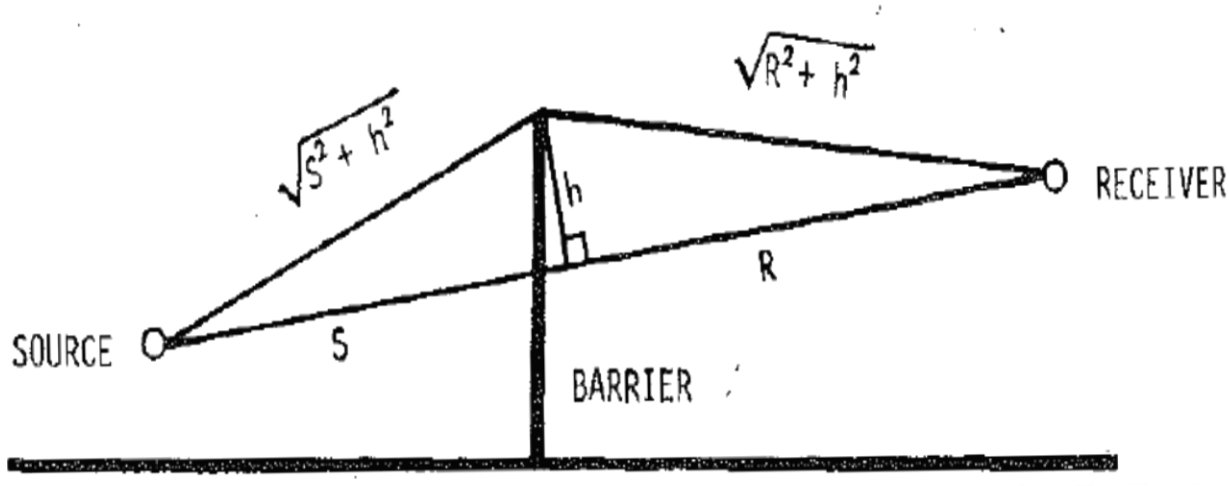

Figure 3.2. Parameters affecting the noise attenuation provided by semi-infinite barriers [2,3]

3.2.2 Noise Attenuation from Finite Barriers

The noise attenuation obtained using finite barriers is based on the same basic principle of diffraction theory. The important difference in this case is that sound waves also bend around the side edges of the barrier as opposed to only bending over the top of the barrier. Therefore, in this case, the length of the barrier also becomes an essential parameter that directly impacts noise attenuation.

The concepts of path difference and Fresnel number based on discussions by Maekawa also apply to finite barriers. However, this concept has to be expanded to correspond to the differences in geometry associated with finite barriers. The studies performed by Moreland and Musa offer valuable insight in understanding the theoretical considerations in determining IL based on diffraction theory [4].

The mean squared sound pressure at a particular point before barrier insertion is approximately given by [11]:

$$|p_0|^2 = \rho c W \left(\frac{Q}{4\pi r^2} + \frac{4}{S_0 \alpha_0}\right) \qquad Pa^2 \qquad (3.6)$$

where,

ρc = characteristic impedance of air (rayls)

W = power of sound source (W)

Q = directivity factor (unitless)

r = distance from the source to the receiver (m)

α_0 = mean sabine absorption coefficient of the room (unitless)

S_0 = total room surface area (m^2)

Once the barrier is inserted between the source and the receiver, the mean squared pressure levels are affected due to the diffraction of sound around the barrier. Observations made by Maekawa, Moreland, and Musa suggest that the mean squared sound pressure at the receiver location can be expressed as [4]:

$$|p_d|^2 = |p_f|^2 \frac{1}{3 + 20\,N_1} \qquad Pa^2 \qquad (3.7)$$

where,

$|p_d|^2$ = mean squared sound pressure level at the receiver location due to diffraction of sound waves over the top of the barrier (Pa^2)

$|p_f|^2$ = free field mean squared sound pressure at the receiver before inserting the barrier (Pa^2)

N_1 = Fresnel number for the diffraction path over the top of barrier

Equation 3.7 represents the mean squared pressure at the receiver exclusively due to diffraction over the top of the barrier. For finite barriers, the rms pressure at the receiver due to diffraction along the side edges would also have to be considered and its contribution would be similar to Equation 3.7 with a Fresnel number for the particular path difference. Consequently, the overall mean squared pressure due to diffraction, which is a summation of all the diffracted paths, can be expressed as:

$$|p_d|^2 = |p_f|^2 \left[\frac{1}{3 + 20\,N_1} + \frac{1}{3 + 20\,N_2} + \frac{1}{3 + 20\,N_3}\right] \qquad Pa^2 \qquad (3.8)$$

$$|p_d|^2 = |p_f|^2\, D \qquad Pa^2 \qquad (3.9)$$

where,

$$D = \sum \frac{1}{3 + 20\,N_i} \qquad unitless \qquad (3.10)$$

Figure 3.3 shows the contribution of three paths and Fresnel numbers in measuring the mean squared pressure at the receiver.

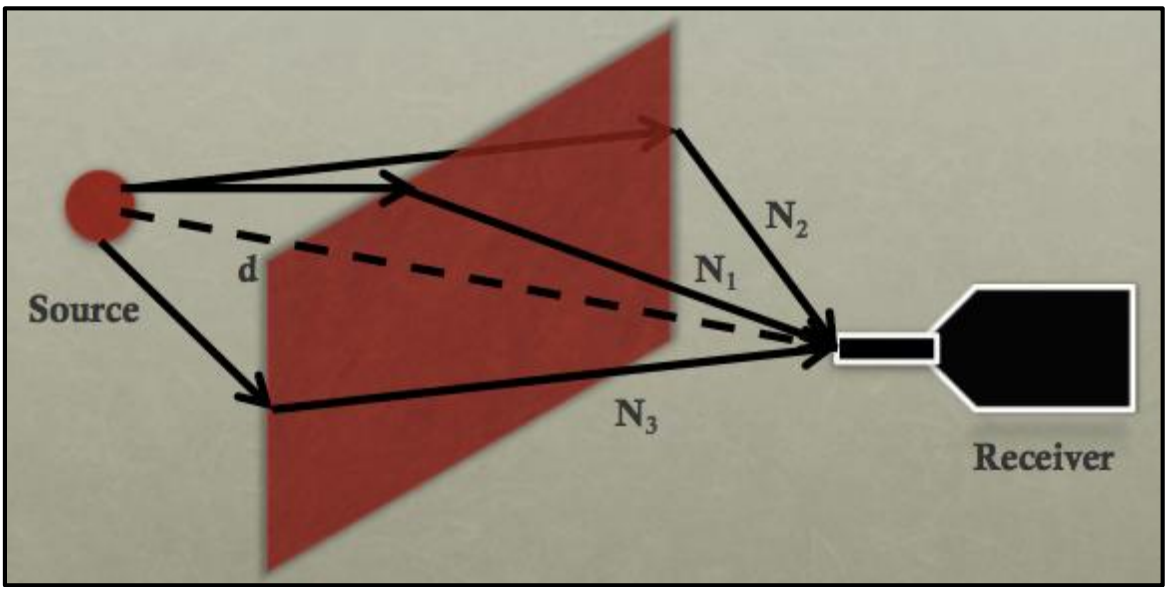

Figure 3.3 Diffraction around a finite barrier affecting the SPL at the receiver [6]

Considering various parameters affecting the overall noise attenuation after barrier insertion, the total mean squared sound pressure at the receiver can be expressed as [4]:

$$|p|^2 = \rho c W \left[\frac{QD}{4\pi r^2} + \frac{4\,K_1 K_2}{S\,(1 - K_1 K_2)}\right] \qquad Pa^2 \qquad (3.11)$$

where,

$$K_1 = \frac{S}{S_1 \alpha_1 + S} \qquad unitless$$

$$K_1 = \frac{S}{S_2 \alpha_2 + S} \qquad unitless$$

S = open area between the barrier perimeter and the room walls, floor and ceiling (m^2)

S_1 = surface area in the source side of the room (m^2)

α_1 = mean absorption coefficient for the source side of the room (unitless)

S_2 = surface area in the receiver side of the room (m^2)

α_2 = mean absorption coefficient for the receiver side of the room (unitless)

The insertion loss due to the finite barrier is defined as [4]:

$$IL_d = 10\ log_{10}\ \left|\frac{p}{p_0}\right|^2$$

$$IL_d = 10\ log_{10}\left[\frac{\frac{QD}{4\pi r^2} + \frac{4K_1K_2}{S\ (1 - K_1K_2)}}{\frac{Q}{4\pi r^2} + \frac{4}{S_0\alpha_0}}\right] \qquad dB \qquad (3.12)$$

If the source and receiver side of the rooms are nearly perfectly absorbing before and after barrier insertion, the complex form of Equation 3.12 can be significantly reduced. In such a case, especially when S is much smaller than S_1 and S_2, we can say that $K_1 - K_2 \approx 0$ and $S_0\,\alpha_0 >> 4$. Therefore, Equation 3.12 can be reduced to:

$$IL_d = 10\ log_{10}\ (D) \qquad dB \qquad (3.13)$$

3.3 Transmission Loss

3.3.1 Transmission Coefficient

The core idea of TL identifies and measures the loss of acoustical power as sound waves transmit through a wall or panel that separates two acoustical spaces. The incident sound waves lose their intensity as they travel through the wall, which leads to a lower sound level on the transmitted side. The fundamental concept of TL is defined using the transmission coefficient τ, which is the ratio of the sound power transmitted through the wall to the sound power incident on the wall. The transmission coefficient is mathematically described as [2],

$$\tau = \frac{W_t}{W_i} \qquad unitless \qquad (3.14)$$

where,

W_t = transmitted sound power (W)

W_i = incident sound power (W)

The transmission coefficient described in Equation 3.14 is more useful when described in terms of sound pressure. Acknowledging the direct proportionality between sound power, sound intensity, and sound pressure, Equation 3.15 could also be expressed as [11,12],

$$\tau(\theta) = \frac{I_t}{I_i} = \frac{|p_t^2|}{|p_i^2|} \qquad unitless$$

$$= \left\{ \left[1 + \eta \left(\frac{\omega \rho_s}{2\rho c} \cos\theta \right) \left(\frac{\omega^2 B}{c^2 \rho_s} sin^4\theta \right) \right]^2 + \left[\left(\frac{\omega \rho_s}{2\rho c} \cos\theta \right) \left(1 - \frac{\omega^2 B}{c^4 \rho_s} sin^4\theta \right) \right]^2 \right\}^{-1} \qquad (3.15)$$

where,

I_t = sound intensity transmitted (W/m^2)

I_i = sound intensity incident (W/m^2)

p_t = sound pressure transmitted (Pa)

p_i = sound pressure incident (Pa)

θ = angle of incidence (rad)

η = composite plate loss factor (unitless)

ρ_s = plate surface density (kg/m^2)

B = plate bending stiffness per unit width (N/m)

ρ = density of medium (kg/m^3)

c = speed of sound in medium (m/s)

Equation 3.15 shows that the transmission coefficient is a function of θ because TL has a strong dependence on the angle of incidence. Expressing the transmission coefficient in terms of sound pressure is useful, however, in its current form, the above equation does not offer many practical advantages. TL can be expressed in terms of the transmission coefficient by averaging τ over all angles of incidence [2]. The expression of TL is logarithmic which makes it practical and comparable to L_p (SPL). It is defined as,

$$TL = 10\ log\frac{1}{\tau} \qquad dB \qquad (3.16)$$

3.3.2 Limp-wall Mass Law

The limp-wall mass law of transmissions loss considers the surface mass of the wall as the singular factor affecting TL. The basic assumption is that $\omega^2 B/c^4\,\rho_s$ is extremely small (<<1). This assumption eliminates the second term from Equation 3.15, which physically translates to eliminating the plate bending stiffness per unit width from the TL expression. Accepting the above assumption, and combining Equations 3.15 and 3.16, TL can be approximated to be,

$$TL(\theta)\ \approx 10\log\left[1+\left(\frac{\omega\rho_s}{2\rho c}\cos\theta\right)^2\right] \qquad dB \qquad (3.17)$$

Equation 3.17 is called the Limp-wall Mass Law Transmission Loss [2]. It should again be noted that the above equation defines TL as a function of the angle of incidence. Since it is a cosine function, the mathematical expression maintains that TL is highest when the sound waves are incident normal to the wall surface ($\theta = 0^0$), and the TL approaches zero for sound waves parallel to the wall surface ($\theta = 90^0$).

In most practical applications, sound waves would not be incident on the wall from a single angle of incidence. For a wide range of incidence angles, Equation 3.17 seems complicated and does not offer the ability to understand the overall TL for all incident angles. Averaging the above equation over all incident angles provides a reduced, practical, and useful equation for TL, which is not a function of θ and can be expressed as,

$$TL = 20\log\ (f) + 20\log\ (W) - C \qquad dB \qquad (3.18)$$

where,

f = frequency of incident sound (Hz)

W = surface density (lb/ft^2/in. or kg/m^2/cm)

C = 33 (unitless) if W is in lb/ft^2/in.

C = 47 (unitless) if W is in kg/m^2/cm

Equation 3.18 is called the Limp-wall Mass law for Random Incidence [2]. This equation also shows that TL is directly proportional to thickness of the wall, which is clearly observed from the unit of surface density. It should be noted that this theoretical knowledge was one of the fundamental concepts in designing the experiment, which is discussed in the following chapter.

Experimental data generally agrees well with this law except for some particular limitations because of the assumptions involved in deriving the Limp-mass Law of Random Incidence. The assumptions made while deriving this law eliminate the effects of material stiffness on TL, which means that the above law works well only for limp materials such as sheet lead. The limpness or lack of stiffness observed in these materials is due to their molecular structure. However, most materials are not limp, and for a construction material such as plywood, its stiffness properties are expected to have an impact on the TL through the material.

3.3.3 Impact of Material Stiffness

The TL of non-limp materials (most materials) generally experience fluctuations at lower frequencies due to the natural vibrations of the wall at resonant frequencies. If a metal plate is fixed along the edges and struck by a hammer, it creates acoustic tones at its natural frequencies, which also correspond to the natural modes of vibration on the plate. The fluctuations are observed due to the existence of these natural vibratory modes of the wall. At these frequencies, the wall appears to be nearly transparent for an incident wave of the same frequency and the TL approaches zero [2]. The low frequency region where the natural vibratory modes lead to TL fluctuations is called the Stiffness-Controlled Region as shown in Figure 3.4. The fluctuations are more significant in materials that have little internal damping. Therefore, the TL performance can be improved by introducing some damping in the system.

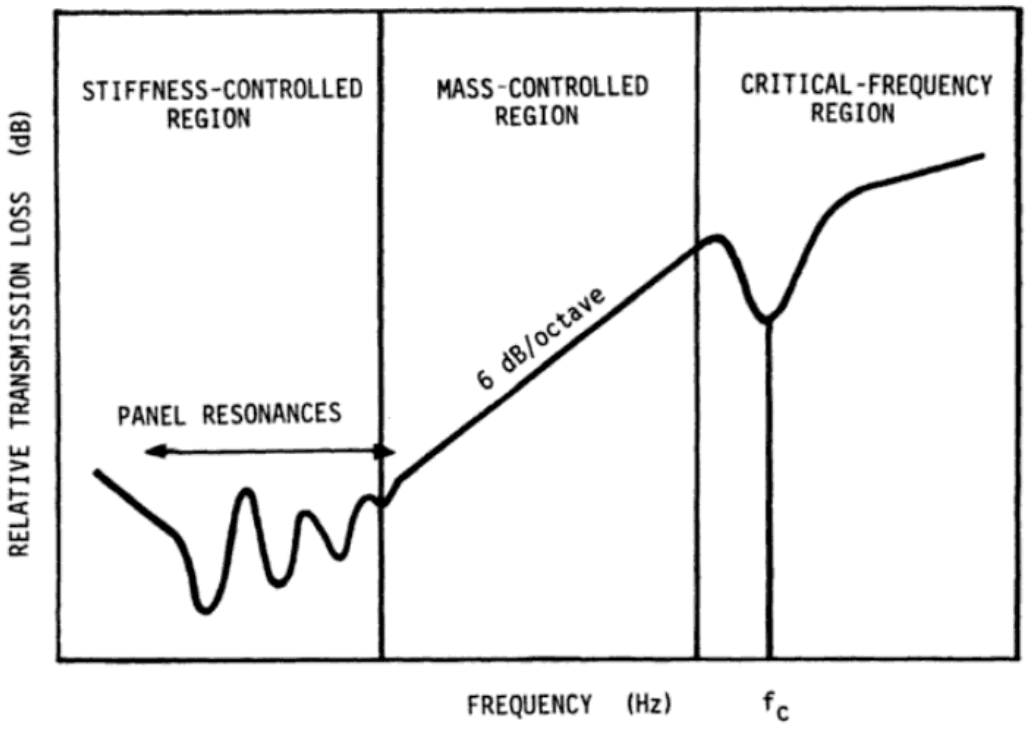

Figure 3.4. TL Frequency response for non-limp (stiffness-dependent) materials [2]

Sound frequencies above the Stiffness-Controlled Region fall under the Mass-Controlled Region as shown in Figure 3.4. As the name suggests, the TL in this region is only mass dependent and generally agrees well with the Limp-wall Mass Law of Random Incidence expressed in Equation 3.18. Analyzing this equation over a range of frequencies and surface densities shows that TL increases at a rate of 6 dB per doubling in frequency or surface density. It can also be observed from Figure 3.4 that TL generally increases for higher incident sound frequencies.

Sound frequencies above the Mass-Controlled Region fall under the Critical-Frequency Region where the Limp-wall Mass Law does not agree well with experimental observations. A resonance like phenomenon is observed in this region at the critical frequency (f_c) as shown in Figure 3.4. This phenomenon is observed when a flexural bending wave is excited and propagates through the wall material. The drop in TL shown in Figure 3.4 is observed if the incident sound waves arrive upon the wall at an angle (θ_i) such that the projection of the sound wave and the flexural wave are in phase [11]. Figure 3.5 shows how an incident sound wave and a flexural wave may interact in a wall. This phenomenon is possible when the following mathematical condition is met,

$$\theta_i = \sin^{-1}\frac{\lambda}{\lambda_f} \qquad rad \tag{3.19}$$

where,

λ_f = wavelength of the flexural wave in the material (m)

λ = wavelength of the incident sound wave (m)

θ_i = angle of incidence (rad)

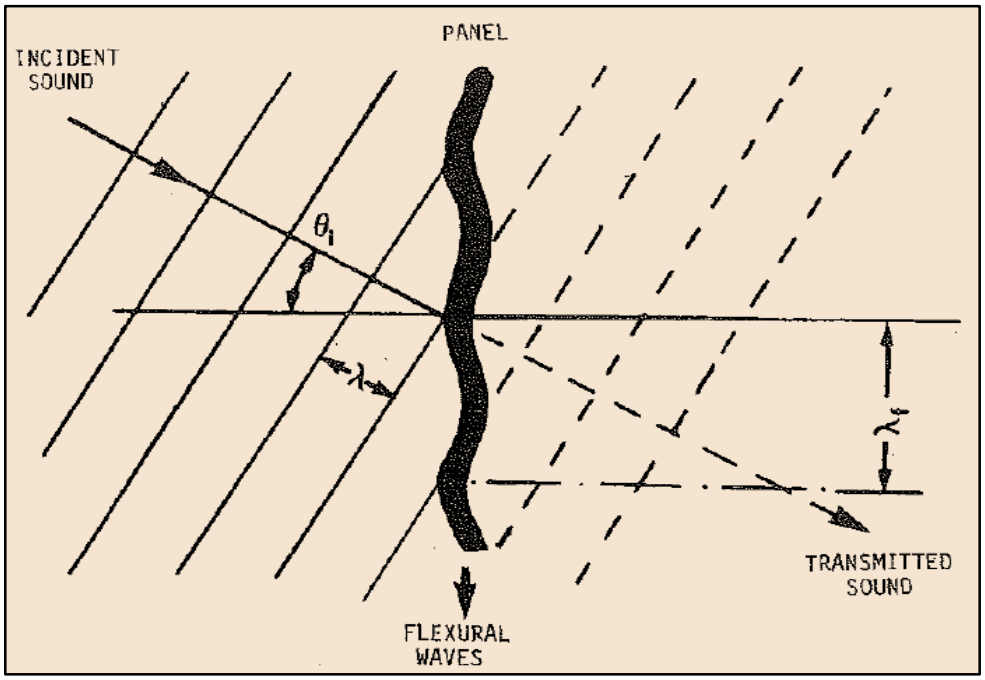

Figure 3.5. A flexural wave and incident sound wave that are in phase [2]

From Figure 3.5, and Equation 3.19, it can be observed that the conditions for f_c can be met over a wide range of frequencies for which the two waves are in phase. However, for most design considerations, only the first order critical frequency is important. For most construction materials, the higher order frequencies are not very interesting since extremely high sound frequencies usually do not pose a noise control challenge. The first order critical frequency can be estimated using the following expression [13],

$$f_c = \frac{c^2}{1.8\, Ut\, sin^2\theta_i} \qquad Hz \qquad (3.20)$$

where,

U = velocity of the flexural wave in the material (m/s)

c = speed of sound in air (m/s)

θ_i = angle of incidence (rad)

t = thickness of material (m)

Equation 3.20 shows that the critical frequency is inversely proportional to the thickness of the wall panel and it also depends on the material of the panel since the speed of sound is dependent on the material of the medium.

3.3.4 Standard Method for Measuring Transmission Loss

The experimental procedure for calculating TL usually follows the ASTM Standard E90, which is the Standard Recommended Practice for Laboratory Measurement of Airborne Sound Transmission Loss of Building Partitions [2]. Figure 3.6 shows an example of such a standard setup. The source room and the receiving room are isolated from each other using a partition. The partition material is the material under investigation for the study of TL. Both the rooms are allowed to be reverberant and a sound source such as a loudspeaker is used to generate sound waves of particular frequencies in the source room. SPL measurements are made in the source room and the receiving room, and the noise reduction (NR) is documented. It can be seen from the above setup that the SPL measured in the receiving room can generally be accepted as a result of sound transmission through the test material. Therefore, the TL can be mathematically defined as,

$$TL = NR + \log\left(\frac{S}{A}\right) \qquad dB \qquad (3.21)$$

where,

S = total area of the sound-transmitting surface of the test specimen (m^2)

A = total absorption in the receiving room (units consistent with S)

NR = $L_s - L_r$, noise reduction between the two reverberating rooms (dB)

The expression in Equation 3.21 only applies to the experimental setup shown in Figure 3.6. Most of the previous TL equations discussed in this section also assume that the TL is a result of a full partition wall between the source and the receiver side. However, this condition is not met while using finite barriers. Despite not meeting these criteria, part of the sound waves incident on the finite barrier are transmitted to the receiver side and the TL is expected to have some impact on the SPL at the receiver. The lack of literature about incorporating the effect of TL on the noise attenuation of finite barriers encourages a focused investigation of this phenomenon.

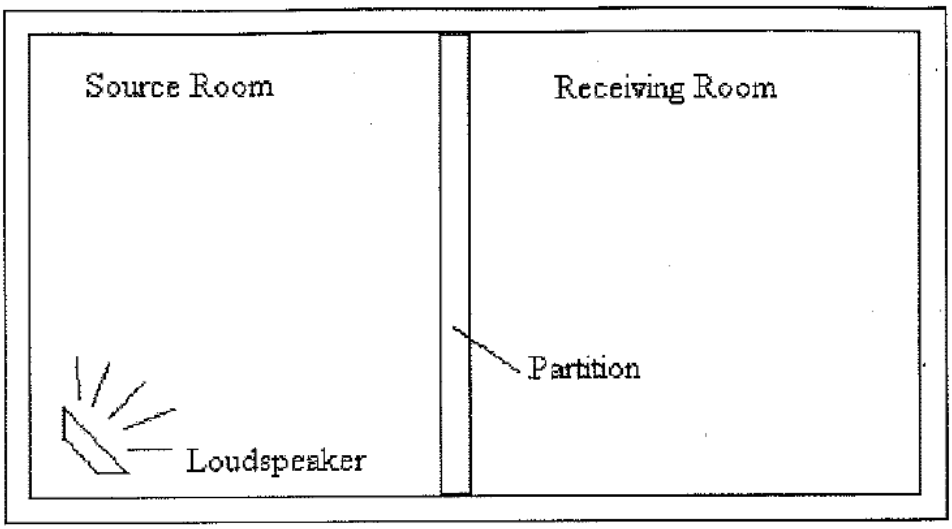

Figure 3.6. Standard setup for measuring TL [14]

3.4 Acoustical Reverberations

3.4.1 Direct and Reflected Sound

The phenomenon of acoustical reverberation is observed when sound is generated in large enclosed spaces. In outdoor environments, SPL can decay freely as the waves travel away from the sound source. However, a sound field that is generated in a closed space is much more

complex, especially when the space is filled with objects that might reflect incident sound waves. An example of such a sound field is shown in Figure 3.7. As seen in the figure, sound experienced in such a space can be divided into two parts, direct radiated sound and reflected sound.

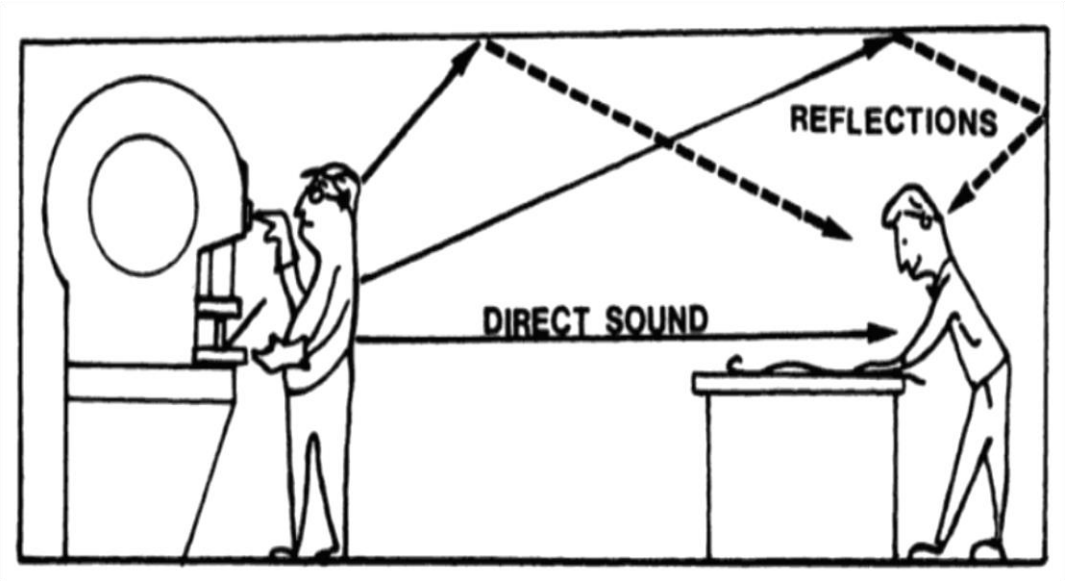

Figure 3.7. Difference between direct sound and reflected sound [2]

The direct sound reaches the receiver along the line of sight while the reflected sound bounces off walls and other reflecting surfaces before reaching the receiver. The path of direct sound may depend on the directivity of the sound source, but the reflected sound arrives at the receiver from multiple directions and is dependent on various factors such as reflecting surface areas, absorption coefficients of walls and objects, etc. For example, surfaces with high absorptive coefficients reduce sound intensity for each reflection off their surface. Therefore, the rate of decay in a reverberant field depends on the number of reflections and the absorptive ability of the surface.

3.4.2 Reverberant Sound Field

Reverberation issues in large enclosed spaces are generally observed as the distance from the source increases. At smaller distances, the direct sound emitting from the source dominates the sound field and this region is called the free field as shown in Figure 3.8. Beyond a certain transition point a reverberant build-up can be observed, and this region is called the reverberant field. The shift from a free field to a reverberant field is gradual and depends on various factors that could affect reverberation. For example, the volume of the room, the directivity of the sound source, and the absorptive capability of the exposed surfaces would all play a vital role in determining the reverberation build-up in an enclosed space.

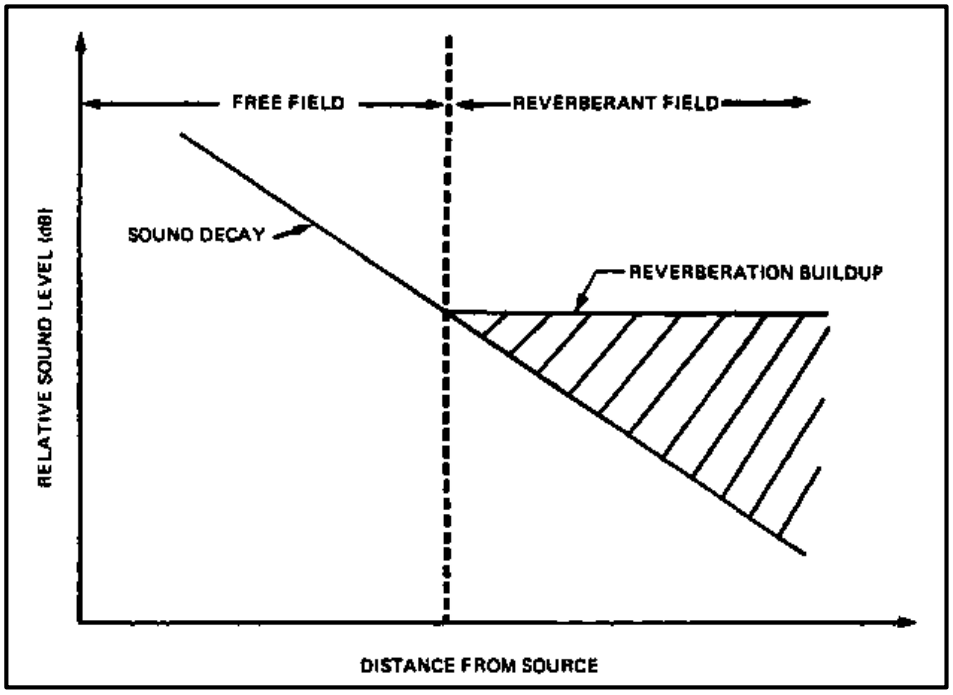

Figure 3.8. Sound fields in an enclosed space [2]

The topic of reverberation control is extremely broad and the theoretical ideas discussed here have also been expressed mathematically. However, the complex mathematical derivations of these ideas are not the focus of this study. Understanding these concepts quantitatively could

be useful but may not have direct applications in offering noise control solutions using finite barriers. However, a qualitative understanding of reverberant sound fields is extremely valuable in studying the behavior of finite barriers in enclosed spaces. This qualitative knowledge was used in the experimental setups for this study and was essential in isolating the TL and diffraction effects of finite barriers from external factors that may affect their performance.

3.4.3 Anechoic Chambers

Anechoic chambers, as the name suggests, are enclosed spaces that do not experience echoes due to reflecting sound waves. They are constructed so that all the walls, ceiling, and floor have an absorption coefficient that is close to 1 (almost completely absorbing) for a wide range of sound frequencies. These surfaces prevent most sound waves from reflecting off their surfaces by absorbing the incident wave energy. Anechoic chambers offer excellent solutions for preventing reverberation build-up in large enclosed spaces, and they are widely used for various noise control studies. For example, noise-generating products such as cars, trucks, motorbikes, and power generators are typically tested in anechoic chambers. The non-reverberating environment allows the investigators to study and map the directivity of sound emitting from a source. The actual source and magnitude of sound levels can therefore be identified, and noise control solutions investigated by studying sound levels in an anechoic chamber. Most manufacturers making products for the heating, ventilation, electric motor, and gas industries provide the customers with octave band power levels for most of their products.

Figure 3.9 shows the anechoic chamber at Orfield Laboratories in south Minneapolis. It has been measured to be 99.99 percent sound absorbent and is also believed to be the “quietest place on earth” [15]. The lowest SPL recorded at Orfield was -8.5 dB which is much below the

threshold of human hearing of 0 dB [5]. As can be seen from the figure, the walls, floors, and ceilings of anechoic chambers are usually treated with wedge-shaped acoustical absorbing material. Fiberglass is a very common absorbing material for such spaces as many studies have found it to be excellent for such applications.

Figure 3.9. The anechoic chamber at Orfield Laboratories [15]

A well-accepted study by Beranek and Sleeper in 1946 found long wedge-shaped structures to be highly effective for absorbing incident sound [16]. Numerous studies since then have found that the shape and size of the wedge plays an important role in widening the range of frequencies that could be absorbed in a chamber. It is usually the low sound frequencies that offer a noise control challenge and are also found to be problematic in anechoic chambers. However, large wedge structures can prove to be effective in absorbing even the lower sound frequencies. The fundamental idea of wedge-shaped absorbing material is that it forces the incident sound waves to bounce off adjacent wedges multiple times which results in the absorption of sound energy and reduces reflections into the room. However, since low

frequencies have large wavelengths, it is important that the size of the wedge is large enough so that these waves can bounce between adjacent wedges. Figure 3.10 provides a useful guideline for choosing fiberglass wedge sizes in order to achieve the desired noise absorption at low frequencies [16]. For example, to achieve adequate absorption for frequencies above 50 Hz, the length of the wedge (L_1) needs to be greater that 53 in.

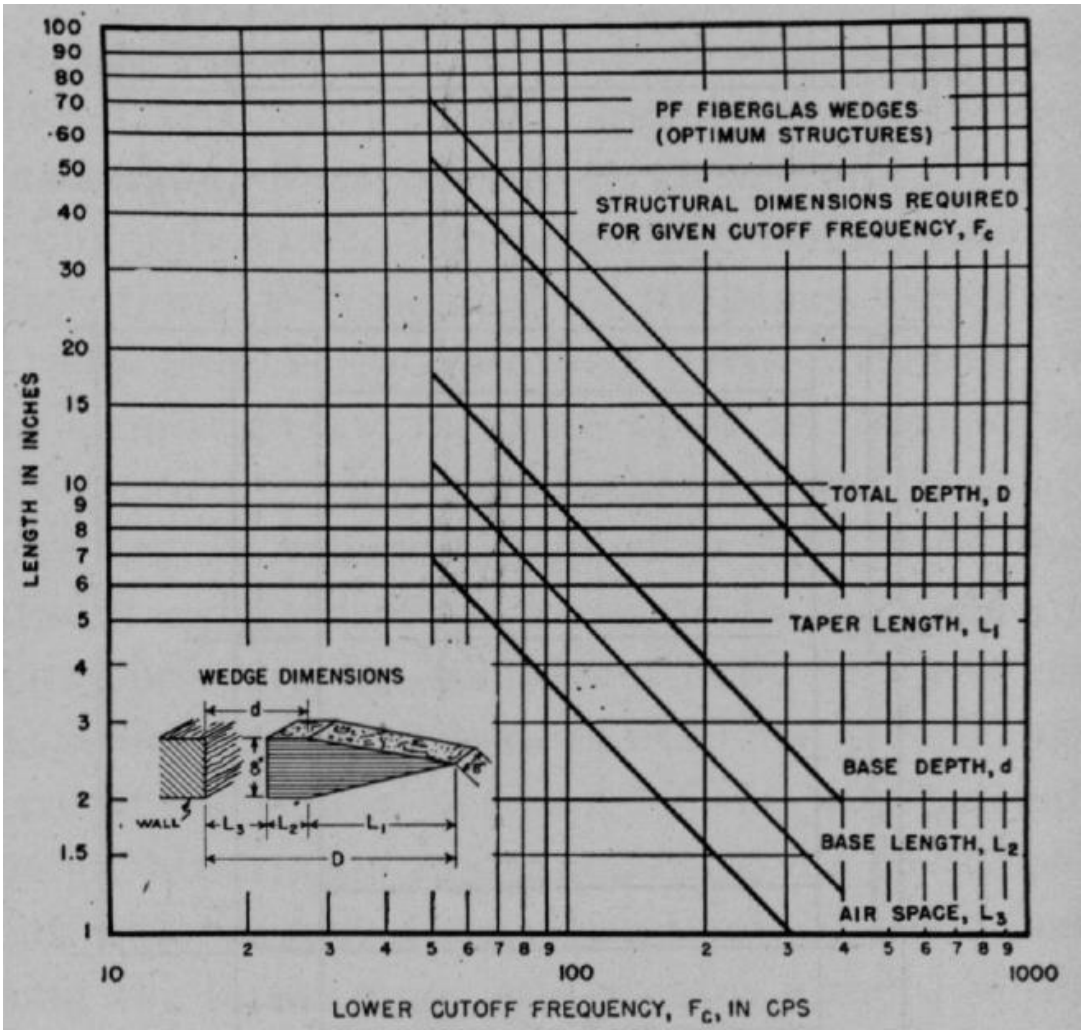

Figure 3.10. Guideline for designing acoustical wedges in anechoic chambers [16]

3.5 Methods for Evaluating Barrier Insertion Loss

3.5.1 Experimental Measurements

The American National Standard and the Draft International Standard provide detailed descriptions for measuring IL due to barriers. A Direct Measurement Method is recommended as it is widely accepted to be the most accurate way of measuring IL [8]. It is possible to use this method in scenarios where the barrier is easily movable or has not been constructed yet. The SPL is measured at a particular reference point before and after the barrier is placed between the source and the receiver. It is essential that the source and receiver locations remain constant for the 'before' and 'after' measurements. This method provides the most realistic and useful way of determining the noise attenuation performance of a barrier.

An alternative method is the Indirect Measurement Method, which is recommended for scenarios where the barrier has already been constructed and is not easily portable [8]. SPL measurements are not possible for the 'before' barrier insertion case but it is still recommended to obtain the 'after' barrier insertion SPL. The 'before' condition is simulated by making measurements at a location that is equivalent to the actual site under consideration.

The American Standards provide another alternative method, which is not included in the Draft International Standards. The Indirect Prediction Method can be used if an equivalent site is not available for the 'before' condition measurements [8]. As the name suggests, the SPL before barrier insertion is predicted, but the precision of the resulting IL can be fairly low.

3.5.2 Numerical Estimation: Ray Tracing Method

The Ray Tracing Method is one of the most commonly used techniques to estimate sound power levels and other acoustic performance parameters. In this method, sound is considered to

be composed of rays that carry sound energy and the wave nature of sound is ignored. It is usually used for understanding sound levels in enclosed spaces with complex reverberant geometries [5].

The method models rays such that they propagate at the speed of sound. As they collide onto the objects or surfaces within the enclosed area, they lose some of their energy. The loss in sound energy depends on the absorption coefficients of the objects. The rays also lose energy due to the resistance offered by the medium. At a particular receiver point, the total energy received from the rays can be computed to estimate the overall sound level at that location [17]. Reverberation concepts such as reverberation time and mean free path are of critical importance in modeling the behavior of rays. Therefore, the surface areas of exposed objects and their absorption coefficients need to be known and included in the model.

A major advantage of the Ray Tracing Method is that it is a computational simulation and does not require the construction of physical structures to evaluate sound levels. However, there are some significant disadvantages is using this method for evaluating barrier performance. For instance, its fundamental idea of neglecting the wave nature of sound is problematic. Wave dependent concepts of diffraction and interference are vital in estimating SPL at the receiver and evaluating overall barrier performance. The method is also not very effective at low sound frequencies because the wavelengths are too large for their wave nature to be ignored. Additionally, managing long calculation times can be challenging since the models tend to be complex and computationally expensive [17].

Chapter IV: THE EXPERIMENT

Barrier IL was obtained by using the Direct Measurement Method described in the previous chapter. Since this was an open experiment and not an existing case study, there was an opportunity to design the necessary conditions for making SPL measurements with and without the barrier. Various aspects of the designed experiment are discussed below.

4.1 The Fresnel Number Concept

The experiment for this study was based on the concept of Fresnel numbers for predicting the theoretical IL of barriers, which was implemented by Moreland and Musa as described in the previous chapter. The foundation of the experiment is based on the idea that the theoretical IL for finite barriers depends only on Fresnel numbers, and should therefore remain constant if the Fresnel numbers remain constant. In practice, the transmission of sound through the barrier is expected to affect the overall noise attenuation, and this idea is tested through experimentation by incrementing the thickness of the barrier. These modifications are expected to maintain constant Fresnel numbers because the path for sound diffraction remains the same. Additionally, based on the theory of TL discussed previously, these modifications are expected to have an impact on TL because wall thickness has a direct impact on TL. The experimental setup attempts to implement this concept to isolate and evaluate the effect of TL on the overall noise attenuation.

4.2 Apparatus

4.2.1 The Sound Source

Figure 4.1. M-Audio BX5n speakers

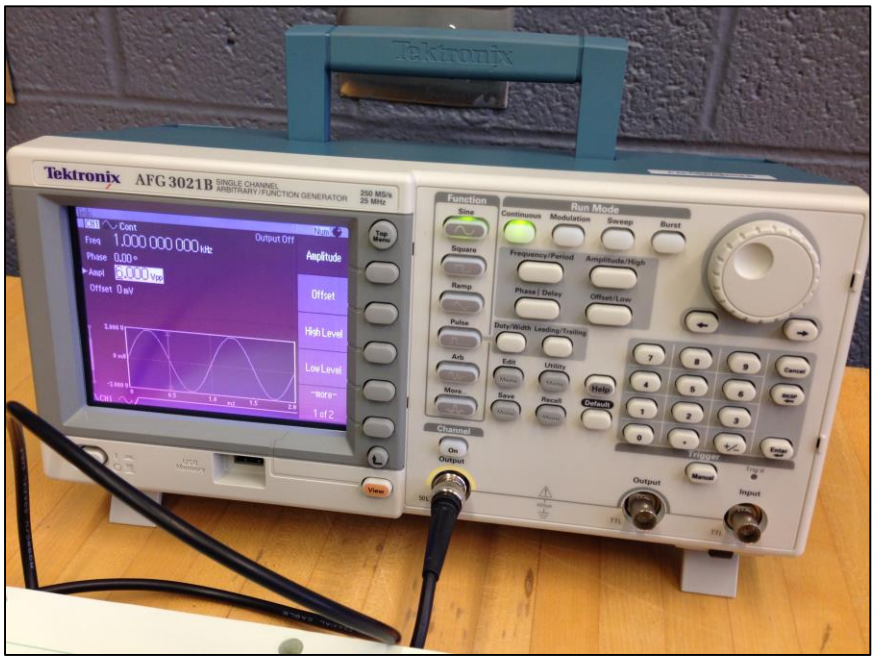

Figure 4.2. Tektronix Function Generator

A M-Audio BX5n speaker, shown in Figure 4.1, was used as the sound source. A Tektronix Function Generator (AFG-3021B), as seen in Figure 4.2, was connected to the speaker using a TRS connector. The function generator was used to create single frequency tones, which was useful in making sound pressure level (SPL) measurements for a range of frequencies.

4.2.2 The Barrier

4 × 6 ft. plywood sheets were used as the sound barrier for the experiment. Each plywood sheet was 0.5 in. thick and a total of three sheets were used for the experiment. The initial measurements were made with one plywood sheet, which provided an initial barrier thickness of 0.5 in., and the successive measurements increased the barrier thickness by 0.5 in. for each measurement.

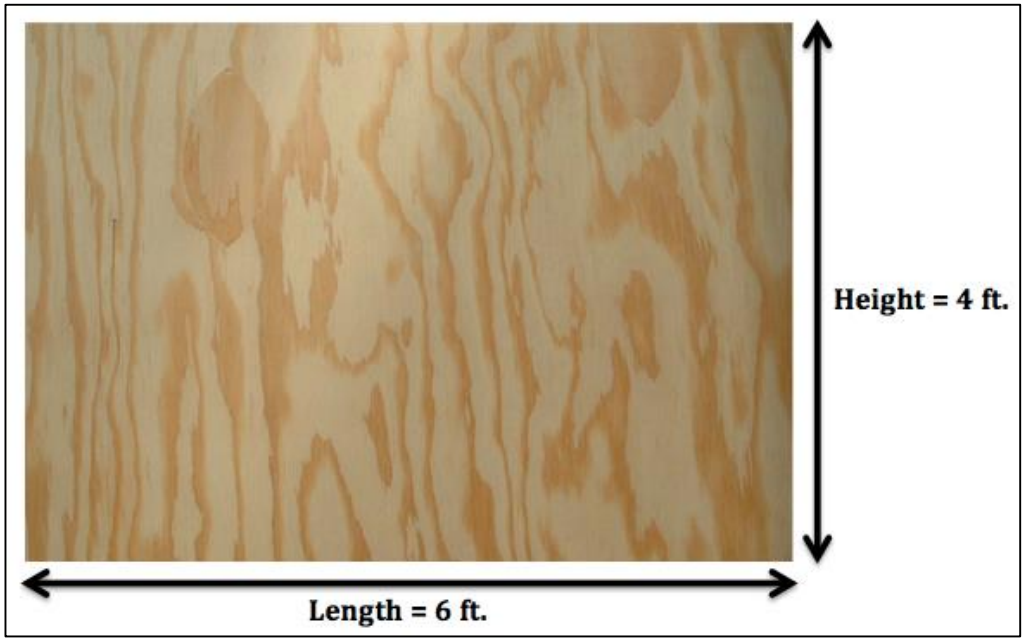

Figure 4.3. 4 × 6 ft. Plywood sheet used as the sound barrier with a 0.5 in. thickness

Plywood was chosen as the barrier material because it is fairly inexpensive. It can be used to make stable and robust experimental setups because it offers considerable mass and stability.

Despite its mass, it is not excessively bulky and does not provide critical challenges in handling and setup modification. Furthermore, plywood is known to provide considerable TL for sound propagating through its thickness. It is an ideal material to study since it is commonly used for construction of indoor fixtures and could be an obvious candidate for designing finite barriers in enclosed spaces.

4.2.3 The Receiver

A NL-04 Rion Integrating Sound Level Meter (SLM), as shown in Figure 4.4, was used as the receiver in the experiment. The SLM has the ability to filter out specific octave or one-third octave bands and measure the SPL for the selected frequency. It is also capable of measuring various decibel-weighting scales and measuring equivalent SPL (L_{eq}) over a period of time.

Figure 4.4. Rion Integrating Sound Level Meter

4.3 Reverberation Control

The experiment was performed at the John T. Meyers Technical Center for Technological Research with Industry at Rose-Hulman Institute of Technology. The acoustic measurements were taken in an enclosed room with an overall volume of approximately 2,200 ft^3. Figure 4.5 shows the dimensions of the room, which has a length of 20 ft., width of 11 ft., and a height of 10 ft. As discussed previously, enclosed spaces are subject to reverberations, and acoustic measurements in a reverberant environment can be distorted as reflected sound is picked up by the receiver along with the direct sound from the source. To address this issue, various reverberation control measures were implemented to improve the accuracy of the data being collected.

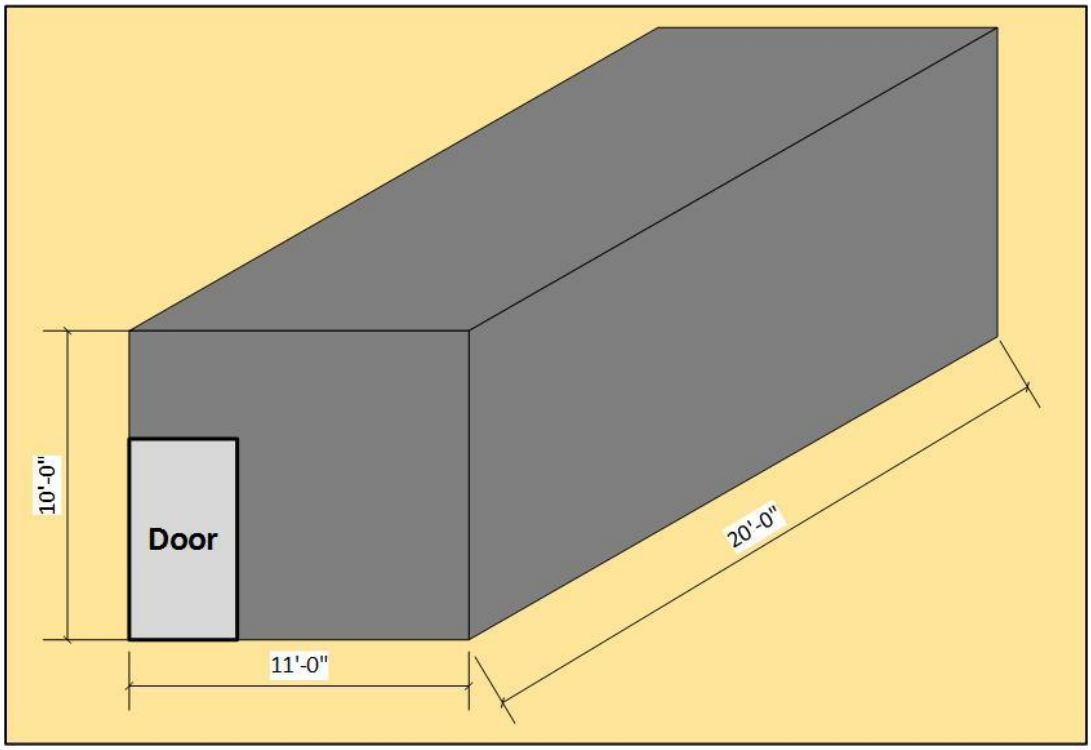

Figure 4.5. Dimensions of the experiment room

Firstly, any objects deemed unnecessary for the experimental setup were removed from the room. Reducing the number of objects in the room reduces the overall area to which sound may be incident. Consequently, the overall reflections in the room were minimal as there was a very small surface area for sound waves to reflect from.

Secondly, the room was used in the form of an anechoic chamber for the experiment. Sheets of absorptive foam with wedges (or cones) were used to achieve anechoic properties for the experiment room. The height of each wedge was 6 in., as shown in Figure 4.6. The ceiling and the four sidewalls were completely covered with the foam while approximately half of the floor area (110 ft.^{2}) was also covered.

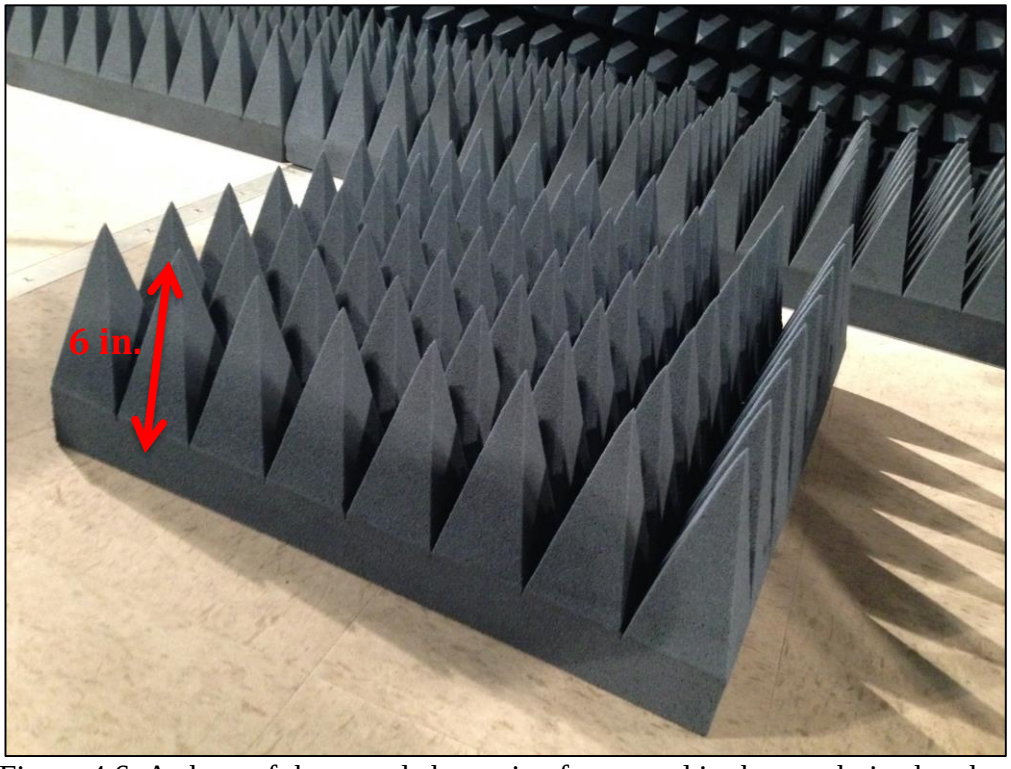

Figure 4.6. A sheet of the sound absorptive foam used in the anechoic chamber

It was not possible to completely cover the entire floor and achieve a perfect anechoic chamber because some surface area had to be left uncovered for the experimental apparatus and

for general movement in order to collect data. However, using such an anechoic chamber without the entire floor being treated is common in making SPL measurements. It dramatically reduces the overall reverberation in the data collection area, and any off-floor reflections that may exist are fairly consistent, which allows accurate understanding of IL from the collected data. The wedges covering the chamber are expected to be particularly effective for higher frequencies, but they are also beneficial in reducing reverberation at lower frequencies. Better reverberation reduction for low frequencies could be achieved by using longer wedges.

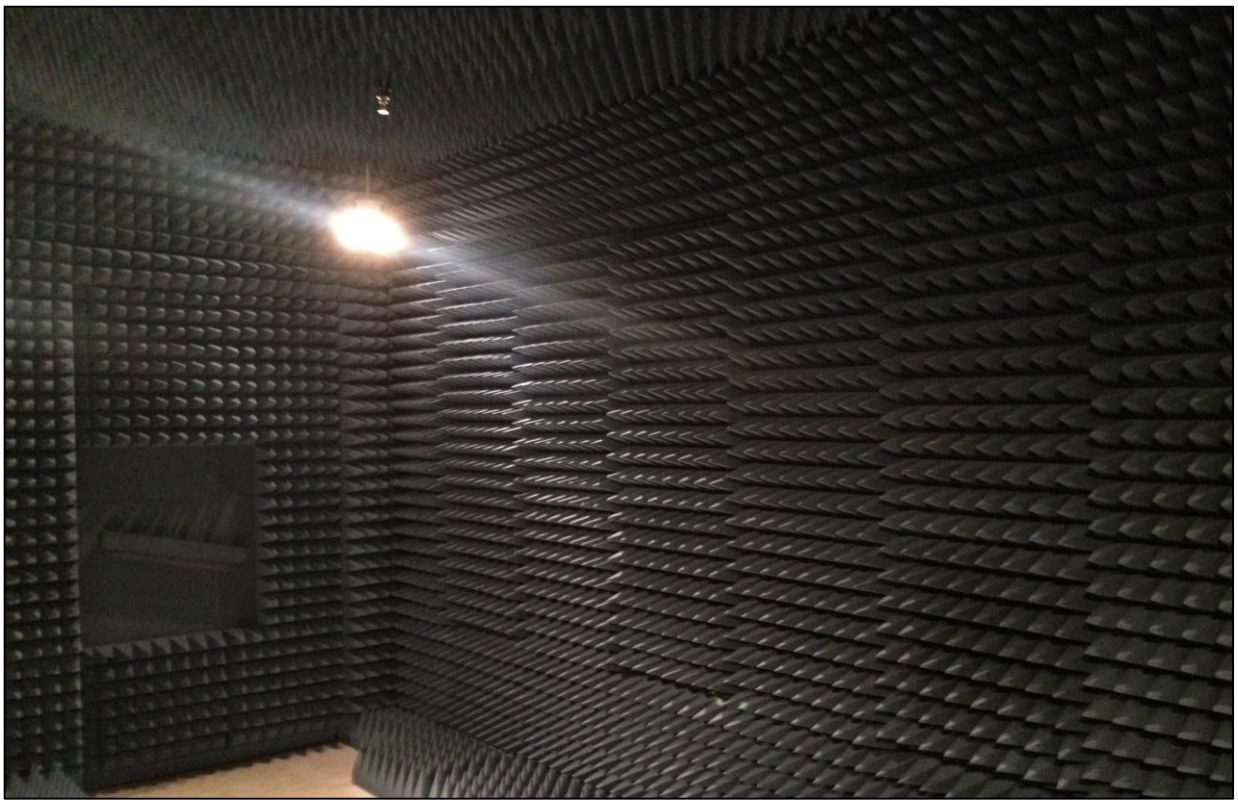

Figure 4.7. The anechoic chamber used to collect data for the experiment

Thirdly, the speakers and the SLM were placed at an appropriate distance from the floor in order to reduce possible sound reflections. It had been observed from previous experiments that proximity of the sound source to the floor could considerably increase reflections and skew SLM readings while measuring SPL [6].

Lastly, the speakers and the SLM were placed in close proximity of each other (~ 6 ft.). As discussed in the previous chapter, reverberation is more prominent in an enclosed space as the distance from the source increases. At smaller distances, the direct sound is less likely to get distorted by reflections. Since the enclosed space is an anechoic chamber, reverberation issues were not expected, but this additional measure was taken to further improve the accuracy of the data collection process.

4.4 Setup and Procedure

The 'Direct Measurement' method for obtaining the barrier IL was used for this experiment. As required by this method, the SLM was used to measure the SPL values with and without the barrier. It was imperative that the positions of the speaker and the receiver remained unchanged.

4.4.1 Initial Setup

The speaker was placed on a stool and its height was measured to be 28 in. above the floor. Such an arrangement was used to reduce the off-floor reflections and control overall reverberation. The function generator was placed on a short folding chair that was placed behind the speaker. It was connected to the speaker to generate the required frequency tones.

The SLM was mounted to a tripod and was fixed at a distance of 6 ft. away from the speaker in the anechoic chamber. It was 26 in. above the floor. The position of the speaker and the function generator remained fixed throughout the data collection process. The SLM was used to make continuous SPL measurements. As discussed in previous chapters, a continuous SPL measurement was more appropriate than L_{eq} measurements because single frequency tones were

being measured and reverberation issues were not expected. No weighting scheme was used for measuring the SPL and standard decibels were chosen as the unit of measurement. A schematic of this arrangement can be seen in Figure 4.8.

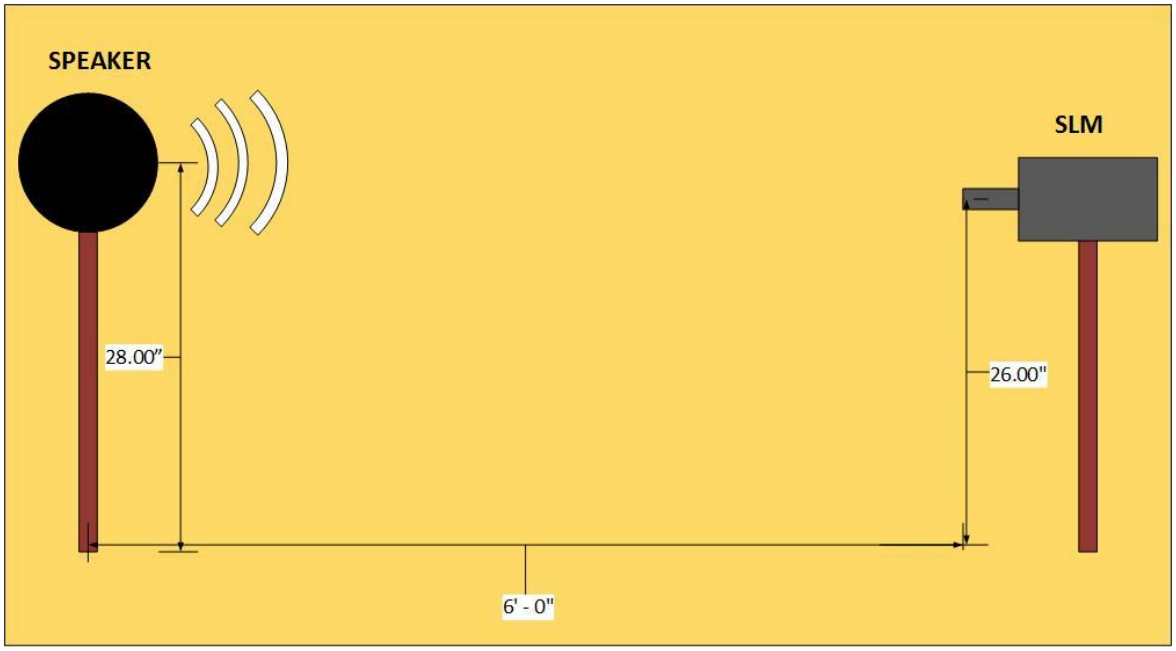

Figure 4.8. A schematic of the experimental setup for SPL measurements before barrier insertion

4.4.2 Ambient SPL Measurements

The SLM was then used to measure the ambient sound levels in the anechoic chamber[2]. Measurements were made using the octave band filter for single center-frequency tones. The SPLs of the center-frequencies for octave bands were measured from 125 Hz to 16000 Hz. These measurements were made to investigate if any external sources of sound were having an impact on the SPL measurements inside the anechoic chamber. It was a preliminary test to observe any unexpected fluctuations or high SPLs that may exist for any of the measured frequencies. These preliminary observations were satisfactory as the SPLs were observed to be fairly low for the center-frequencies.

[2] See Appendix A for specific SPL data for ambient sound

4.4.3 SPL Measurements before Barrier Insertion

These SPL measurements were made using the same setup as the previous ambient SPL measurements. The only difference in this measurement was the use of the frequency generator and speaker to generate single center-frequency tones for each of the desired octave bands. The amplitude of sound controlled by the frequency generator was left constant at 10 V_{pp} and the volume setting on the speaker was also left constant throughout the experiment in order to obtain consistent amplitudes from the sound source for a particular frequency. The octave band filter on the SLM was used again to filter out undesired sound. The SPL measurements were documented and used in the experimental IL calculations[3]. Figure 4.9 shows the setup used for making these measurements.

Figure 4.9. Setup used for making SPL measurements before barrier insertion

[3] See Appendix B for specific SPL data (without a barrier) for the center-frequencies generated using the sound source

4.4.4 SPL Measurements after Barrier Insertion

The barrier, with a thickness of 0.5 in., was placed at a distance of 3 ft. each from the speakers and the SLM. Two wooden legs were attached to each side of the barrier to provide stability to the barrier and maintain a vertically upright position. Figure 4.10 shows a schematic of the experimental setup[4]. Similar to the previous setup, measurements for the same octave band center-frequencies were made while maintaining previous positions and settings of the speaker and the SLM. The SPL measurements were documented for experimental IL calculations.

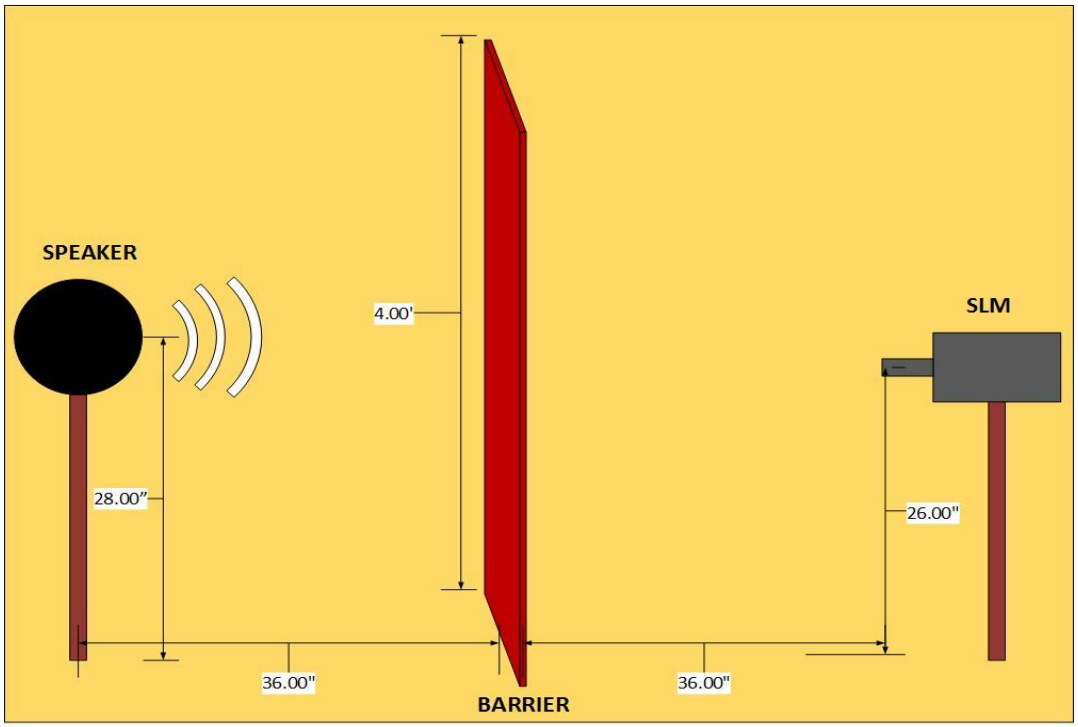

Figure 4.10. A schematic of the experimental setup for SPL measurements after barrier insertion

The barrier was then removed from the anechoic chamber and modified by connecting an identical plywood sheet to the existing one to obtain a barrier with the same surface area and an increased thickness of 1 in. The above-mentioned procedure for SLP measurements was repeated for this modified barrier.

[4] See Appendix C for images of the experimental setup for SPL measurements made using a barrier

The barrier was further modified by attaching another plywood sheet to the existing barrier to obtain an overall barrier thickness of 1.5 in. The entire data collection process was repeated for this modified barrier[5].

Due to some observations made at the 4000 Hz sound frequency that will be discussed in the following chapter, additional data was obtained for frequencies between 2000 Hz and 8000 Hz. The one-third octave band filter on the SLM was used to obtain more data points and gain a better understanding of the barrier behavior around 4000 Hz.

4.4.5 Measuring Diffraction Paths for the Sound Waves

The barrier was not placed exactly along its centerline when it was positioned between the speaker and the SLM. The shape of the absorptive foam and its arrangement on the floor meant that the barrier could not be placed along the centerline. While the speaker and the SLM were positioned opposite each other, 28.5 in. of the barrier length lay on the left side of the source and 43.5 in. of the barrier length lay on the right side of the source. The schematic in Figure 4.11 shows this arrangement. This arrangement is not expected to have any negative effect on the collected data as it still fits the Fresnel number diffraction model. The diffraction theory used for calculating IL does not require a symmetric arrangement, and the IL values for the above setup are theoretically acceptable and predictable.

The diffraction paths for the sound waves were measured for this arrangement and used to calculate the theoretical IL values by using the Moreland and Musa literature [4].

[5] See Appendix B for specific SPL data for various frequencies and calculations for experimental IL

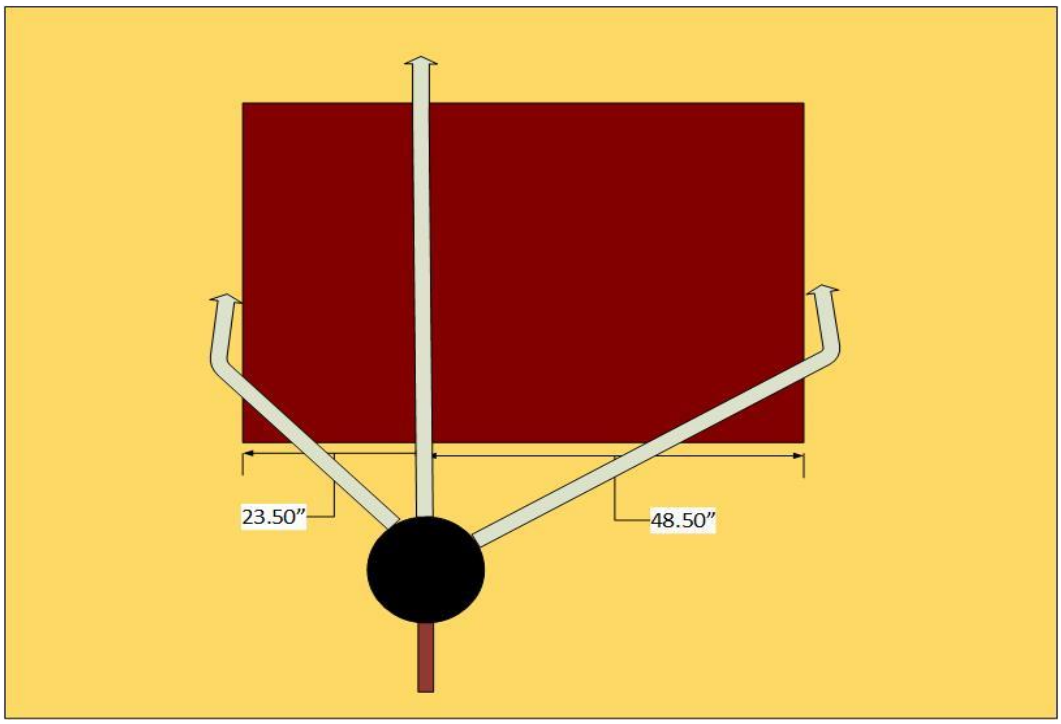

Figure 4.11. A schematic of the acoustic diffraction paths for the experimental setup

4.4.6 Precautions

Any surface exposed to the incident sound increases the possibility of reflecting sound waves in an enclosed space. It was also clearly observed that movements caused fluctuations in the SPL measured at the receiver. Therefore, it was essential to not have any moving bodies or objects in the anechoic chamber while obtaining the SPL data. During each measurement, the author maintained a fixed position behind the SLM from where the SLM display was observable but no movements were necessary to record the SPL values. As an additional precaution, any objects that may produce sound, such as cell phones, and laptops were kept out of the anechoic chamber during the experiment.

Chapter V: RESULTS AND DISCUSSION

5.1 Theoretical Calculation of IL

The theoretical values of IL were calculated using the equation for the IL of finite barriers formulated by Moreland and Musa [4]. This study, which was discussed in detail in Chapter 3, offers the following equation for calculating barrier IL:

$$IL = 10\ log_{10}\ (D) \qquad dB \qquad (5.1)$$

where,

$$D = \sum \frac{1}{3 + 20N_i} \qquad unitless \qquad (5.2)$$

and N_i is the Fresnel Number for the particular path under consideration.

From the review of similar studies and the theory of diffraction, it was expected that the barrier IL would increase with increasing frequencies. Figure 5.1 shows the theoretical values of IL for the barrier and setup used for experimental SPL measurements. Equation 5.1 was used to calculate the IL for the source frequencies used for collecting experimental data. Therefore, the theoretical calculations agree with the basic principle of diffraction theory, which expects higher IL for higher source frequencies[6].

[6] See Appendix D for detailed calculations of theoretical IL

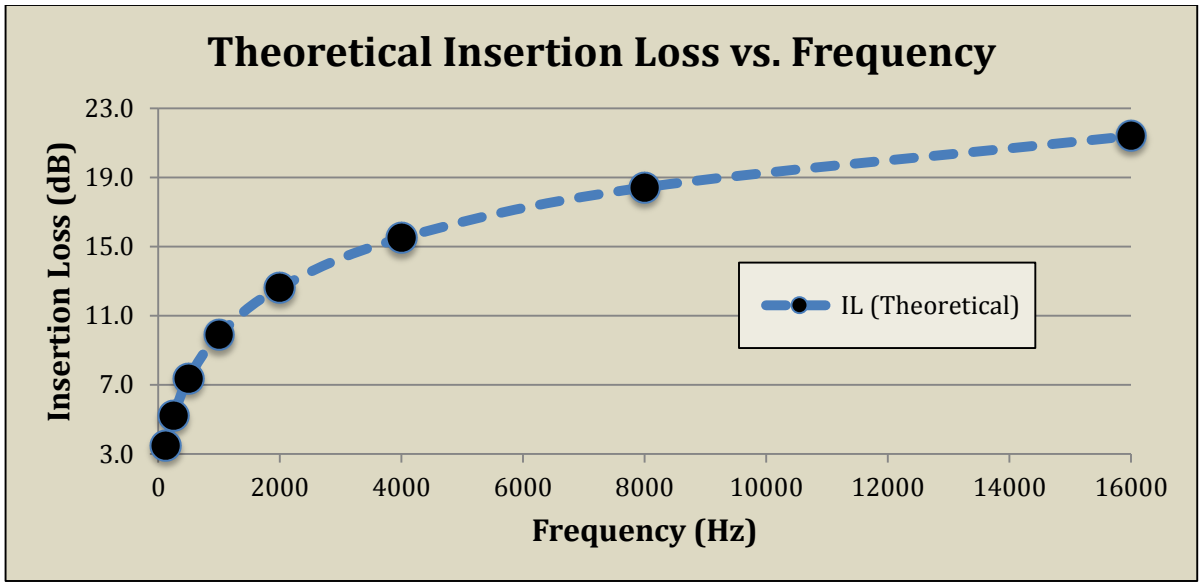

Figure 5.1. Theoretical IL for the experimental setup used in this study

5.2 Comparing Theoretical Calculations to Experimental observations of IL

Using the experimental SPL values documented from the data collection process, the experimental IL was calculated as the difference between the SPLs before and after barrier insertion:

$$IL = SPL_{no\ barrier} - SPL_{with\ barrier} \qquad dB \qquad (5.3)$$

The experimental observations were compared to the expected theoretical calculations. This comparison provides some valuable insight about the physical behavior of sound waves when a barrier obstructs their travel paths.

5.2.1 Barrier Insertion - 0.5 in. Thickness

Figure 5.2 shows the comparison of the experimental IL observations to the theoretical predictions for the first set of data using the 0.5 in. thickness barrier. It was observed that the experimental IL generally agrees with the diffraction theory, and increases with increasing sound frequencies. Figure 5.2 also shows that for this particular barrier thickness, the IL values are

generally similar to or lower than the expected theoretical values. In contrast to diffraction theory, the IL values at 250 Hz, 500 Hz, and 4000 Hz were observed to provide considerably lower noise attenuation as opposed to the expected gradually improving performance for successively higher frequencies. The trough in the curve observed at 4000 Hz was particularly prominent and the difference between the predicted and experimental value was 8.9 dB (approx. 57%). This observation provides some evidence of the impact of TL on the overall IL and will be further discussed later in the chapter.

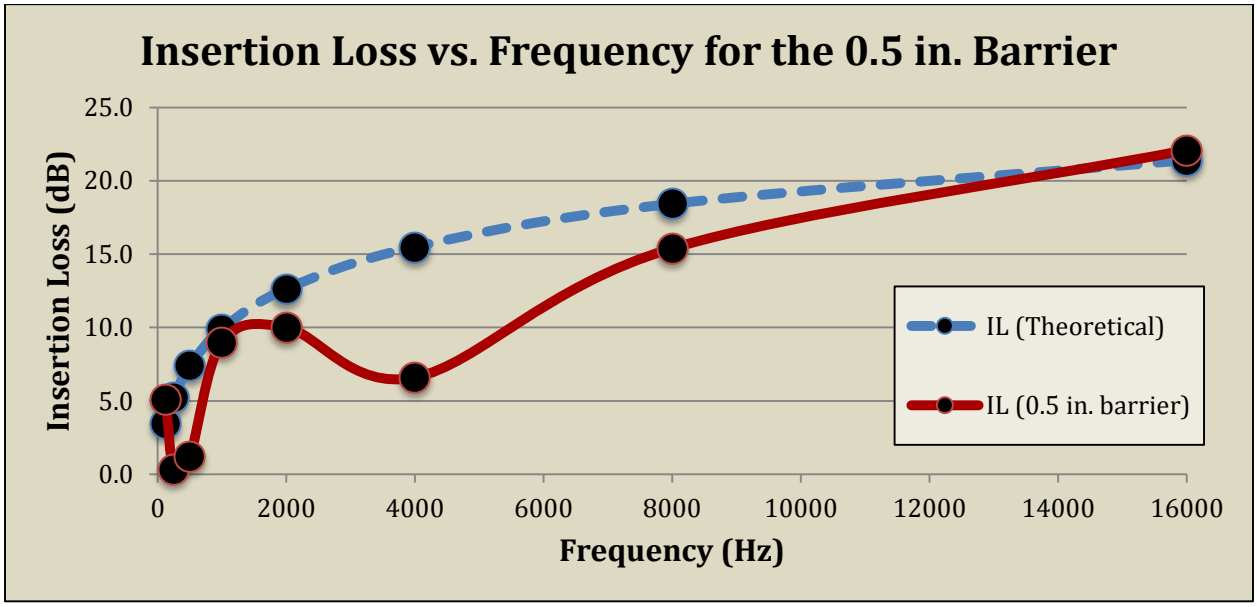

Figure 5.2. Comparison of theoretical IL to experimental observation for the 0.5 in. barrier

5.2.2 Barrier Insertion - 1.0 in. Thickness

Figure 5.3 shows the comparison of the experimental IL observations to the theoretical predictions for the second set of data using the 1.0 in. thickness barrier. This set of experimental measurements was also observed to generally agree with diffraction theory. In general, the experimental values were in close proximity with the theoretical predictions, which suggests slightly higher IL values as compared to the previous setup. A notable exception to the Moreland and Musa prediction is the IL measured at 16 kHz, which was considerably larger. The

difference between the predicted and measured values was 6.6 dB (approx. 31%). This was a particularly interesting observation because the experiments conducted by Moreland and Musa compared the IL measurements to the theory only until a frequency of 8000 Hz [4]. This could possibly indicate the departure of experimental situations from diffraction theory at very high source frequencies. The anomalies noted at 250 Hz, 500 Hz, and 4000 Hz for the previous setup were observed to repeat themselves. The IL loss at 4000 Hz was considerably lower than expected again. The difference in the SPL was 7.8 dB (approx. 50%). The overall significance of TL in these observed exceptions is discussed later in the chapter.

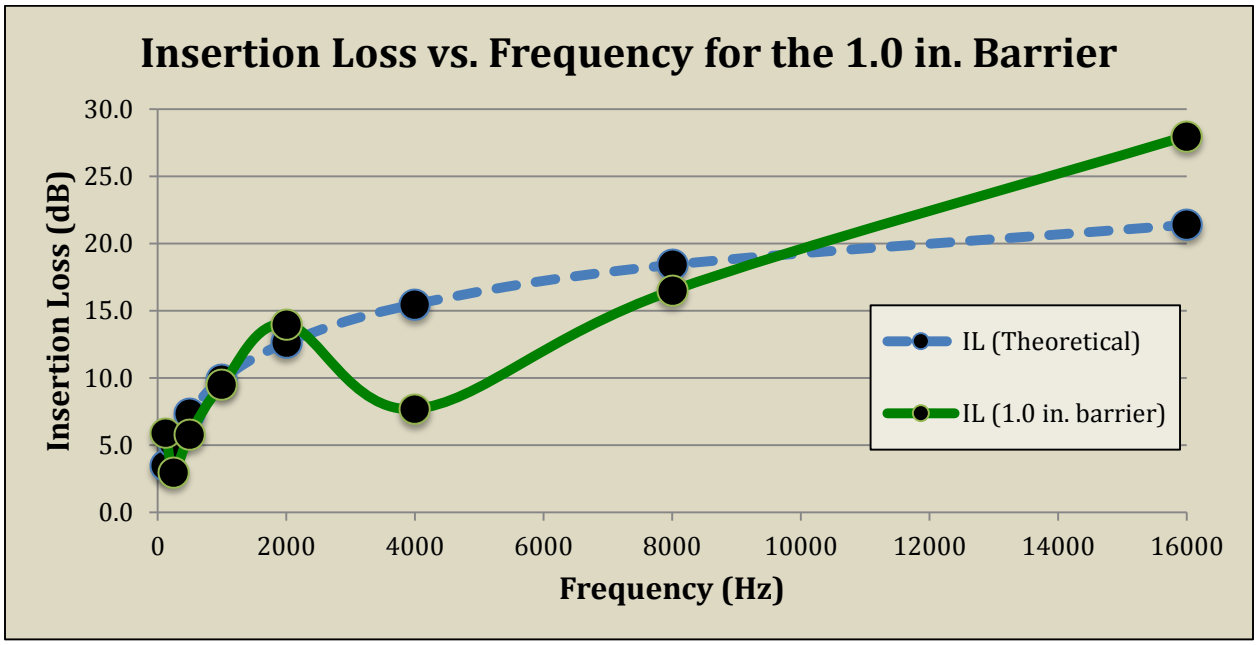

Figure 5.3. Comparison of theoretical IL to experimental observation for the 1.0 in. barrier

5.2.3 Barrier Insertion - 1.5 in. Thickness

Figure 5.4 shows the comparison of the experimental IL observations to the theoretical predictions for the third set of data using the 1.5 in. thickness barrier. As expected from previous observations, this set of measurements also generally agreed with diffraction theory. It was also observed that the experimental IL values were generally similar to or larger than the expected

theoretical values, which suggests slightly higher IL compared to the previous setup. The IL at 16 kHz was once again found to be considerably larger than the predicted value. The difference between the predicted and measured values was 10.7 dB (approx. 50%). The drop in the IL values at 250 Hz, 500 Hz, and 4000 Hz was observed again in this data set and it confirmed a recurring trend in all the experimental setups. However, in this data set, the IL value at 4000 Hz was much closer to the predicted value with a difference of 2.8 dB (approx. 18%). Despite the small difference, this data point is a significant exception to the expected upward trajectory of the IL curve.

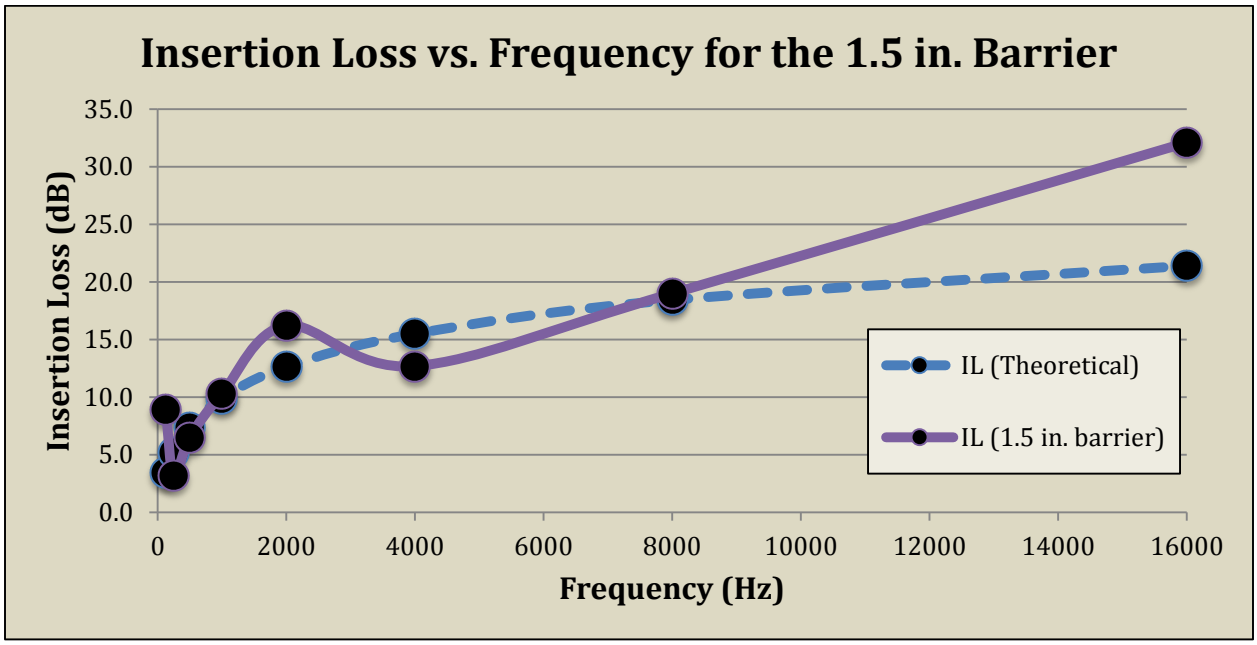

Figure 5.4. Comparison of theoretical IL to experimental observation for the 1.5 in. barrier

5.2.4 Comparative Assessment of all Barrier Setups

Figure 5.5 shows a comparison of the IL values from all the experimental setups and the theoretical predictions. Figure 5.6 communicates the same information for lower source frequencies, but it is magnified for improved visibility because the data points are in close proximity.

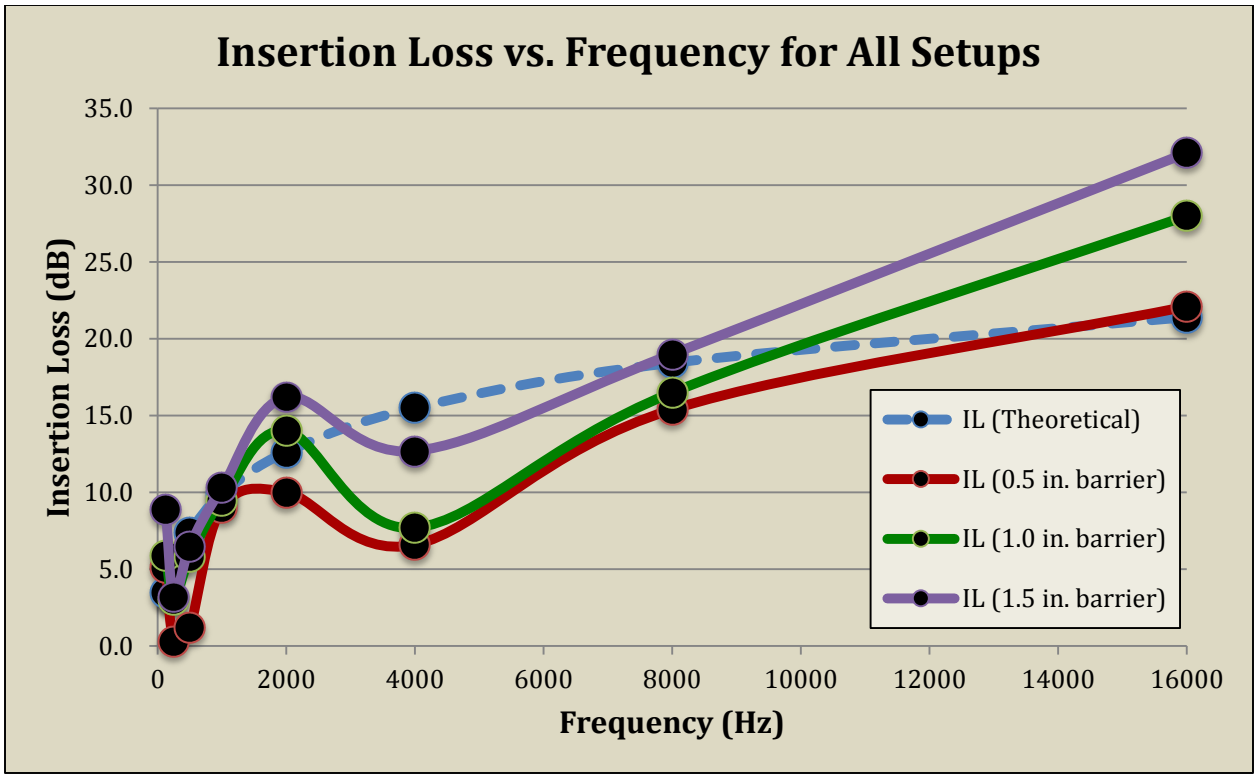

Figure 5.5. Comparison of theoretical IL to experimental observation for all setups

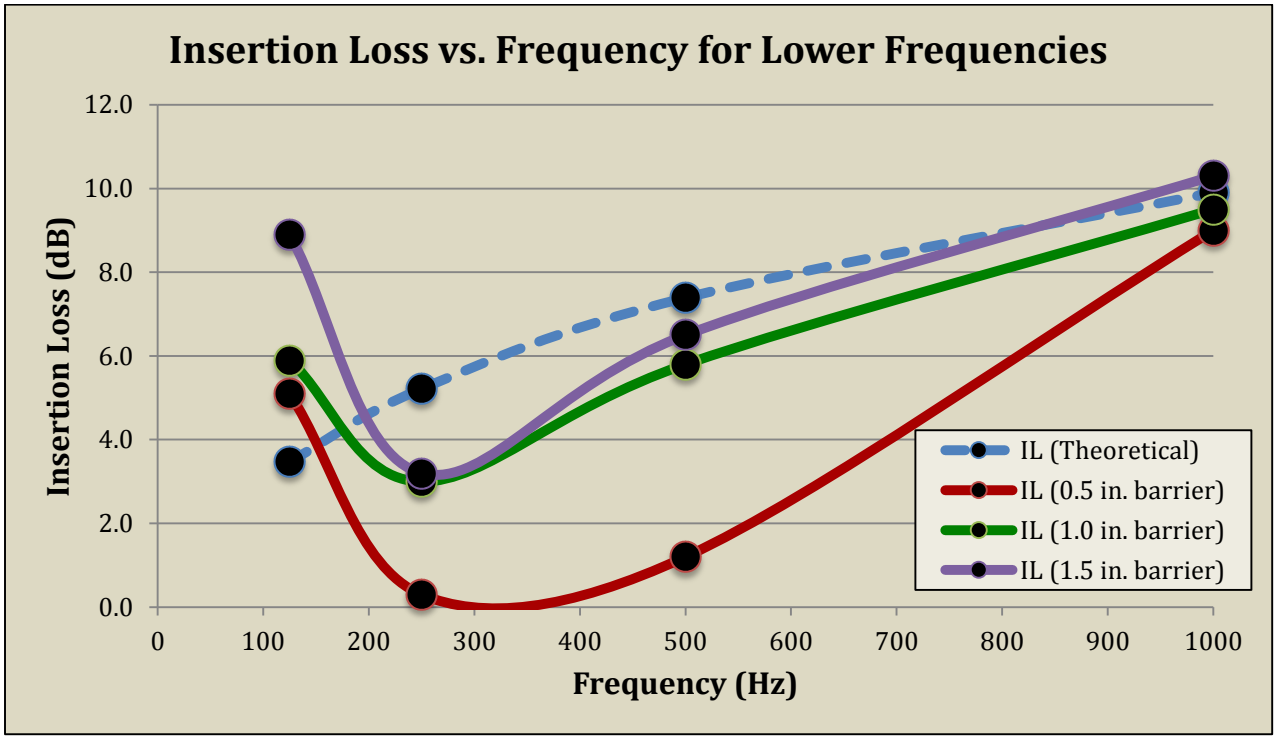

Figure 5.6. Comparison of theoretical and experimental IL at lower frequencies

It can be clearly observed from these plots that the upward trend showed by the experimental curves generally agrees with diffraction theory with the exception of some data points that were previously mentioned. The plots also show that the experimental curves generally converge to the theoretical curve as the barrier thickness is increased from 0.5 in. to 1.5 in. The overall IL values are also observed to increase for the entire frequency range as the thickness of the barrier increases. The important experimental detail of maintaining constant Fresnel numbers and consequently ensuring consistent diffractions through all the setups provides strong evidence of the impact of TL on the overall IL of the barrier. As discussed in Chapter 3, the TL is directly proportional to the thickness of the barrier. The improving IL values for increasing barrier thicknesses recognize this characteristic of TL and they physically represent a smaller number of sound waves being transmitted through the barrier. This observation confirms the hypothesis that TL has a significant impact on the overall IL of finite barriers and encourages specific assessments about the nature of this interdependence.

5.3 Effect of Critical Resonance Frequency of TL on Noise Attenuation

The recurring observation of a considerable drop in noise attenuation at 4000 Hz was investigated in more detail by obtaining additional data points in the frequency range of 2000 Hz to 8000 Hz. Using the center-frequencies of one-third octave bands allowed the collection of additional data points in this frequency range. Figure 5.7 plots the IL measurements for all the experimental setups and compares them to the theoretical predictions. Based on the evidence of the effects of TL observed in Figure 5.5 and 5.6, this observation was reviewed and compared to the TL literature from Chapter 3. The data suggests that source frequencies above 3000 Hz lie in the critical-frequency region for the plywood barriers used in the experiments. Figure 3.7 shows

how noise attenuation due to TL can drop considerably at f_c. The additional data points suggest that f_c for the barrier used in this experiment is approximately 4000 Hz and lies in the one-third octave band from 3548 Hz to 4467 Hz.

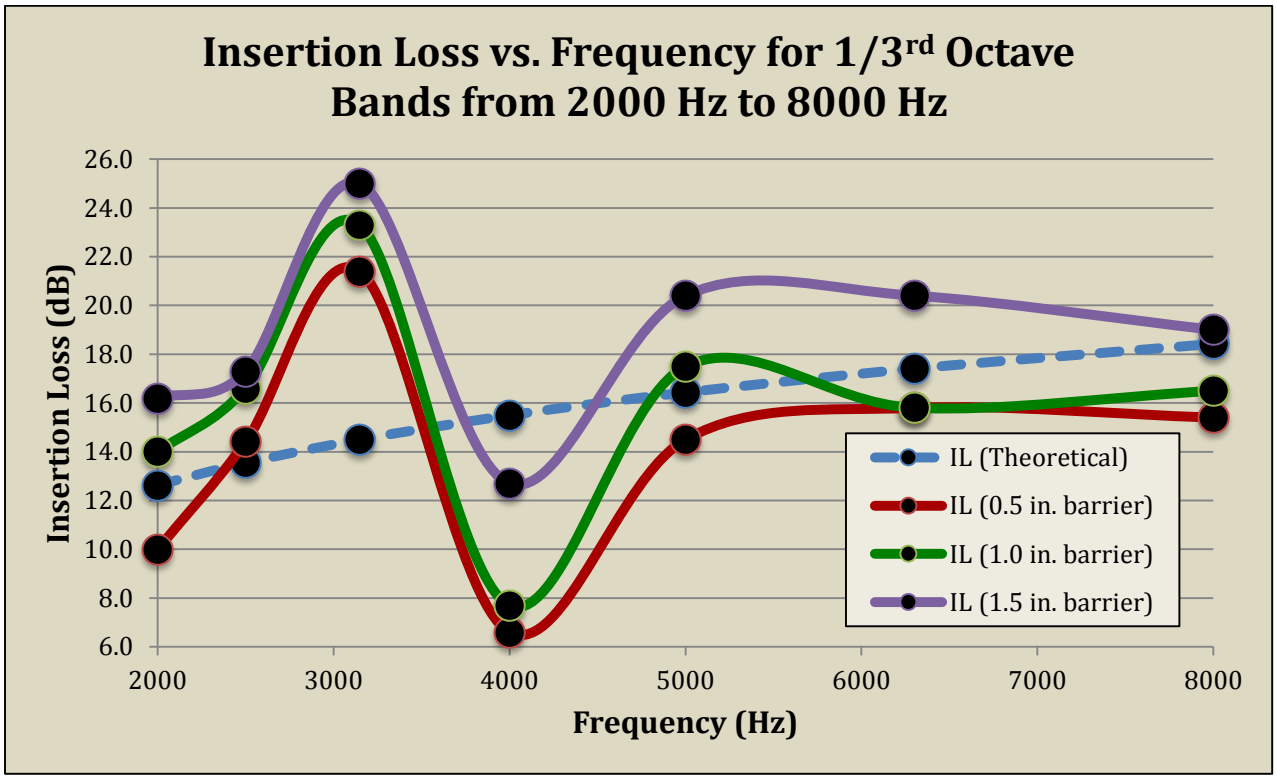

Figure 5.7. Critical resonance frequency of the barriers is observed to be around 4000 Hz

Diffraction theory does not consider the resonance-like effect at f_c, which dramatically reduces the noise attenuation performance of barriers. The critical frequency could prove to be a performance issue if the barrier is designed based on diffraction theory alone and without investigating the source sound frequencies. The overall IL was particularly low (8.6 dB) for the 0.5 in. thickness barrier. An appropriate strategy to tackle such an issue would be to identify the dominating source frequencies and choose the material and dimensions of the barrier to achieve optimum noise attenuation levels. If the noise source has various dominating frequencies, a composite barrier made from two or more elements could be considered. Composite barriers

would offer different TL properties for different materials and the negative impacts of having a singularly dominant f_c could be considerably reduced. In addition to these techniques, the use of absorptive barriers, which was discussed in Chapter 2, could also prove to be an excellent solution due to their ability to minimize sound wave transmission through the barrier.

5.4 Effect of Panel Resonances on TL and the Overall Noise Attenuation

The fluctuations in IL for all the experimental setups observed in Figure 5.6 could also be attributed to TL characteristics. TL generally fluctuates at low frequencies due to natural vibratory resonances of barrier panels. This behavior was discussed in Chapter 3 and Figure 3.7 shows how panel resonances can impact TL. The overall IL was observed to be particularly low at 250 Hz and 500 Hz for the experimental setup with a 0.5 in. barrier thickness. The difference between the predicted value and the experimental measurement was 4.9 dB at 250 Hz and 6.2 dB at 500 Hz, while the overall IL values were 0.3 dB and 1.2 dB respectively. The fluctuations observed in the experimental data suggest that these source frequencies lie in the stiffness controlled region of the barrier panel and provides further evidence of the interaction between TL and diffraction based IL.

It can be observed that panel resonances would be of particular concern to barrier design only if dominant source frequencies are fairly low. In such a situation, it would be appropriate to investigate the natural vibratory modes for the selected material and dimensions of the barrier. An alternative strategy would be to use absorptive material or damping targeted to minimize the transmission of sound at low frequencies and achieve the desired noise attenuation performance through diffraction.

5.5 Effect of Barrier Thickness on Frequency Specific Noise Attenuation

The literature review and experimental observations provide compelling evidence of the frequency dependent nature of noise attenuation. Considering the impact of TL and its direct proportionality to barrier thickness, which was observed in Figure 5.5 and 5.6, it is important to consider how barrier thickness impacts the noise attenuation for specific frequencies. The plots in Figure 5.8 show how the performance of the barrier varies with increasing barrier thickness and also compares this thickness dependent variation to diffraction based theoretical IL, which is not dependent on barrier thickness. The constant Fresnel numbers maintained for all the experimental setups prove that the increasing trend of IL for increasing barrier thickness was exclusively a direct result of increasing and thickness dependent TL. Considering the IL values for the 0.5 in. barrier as a baseline, incremental IL values were calculated for the successive barrier setups. Table 5.1 shows the incremental IL, which physically corresponds to the improvement in TL for each source frequency.

Table 5.1. Incremental improvement in noise attenuation due to improving TL

Octave Band (Hz)	**Center Frequency (Hz)**	**IL – 0.5 in. (dB)**	**Incremental IL – 1.0 in. (dB)**	**Incremental IL – 1.5 in. (dB)**	**Overall Increment at 1.5 in. (%)**
88 – 177	125	5.1	0.8	3.8	74.5
177 – 354	250	0.3	2.7	2.9	966.7
354 – 707	500	1.2	4.6	5.3	441.7
707 – 1414	1000	9.0	0.5	1.3	14.4
1414 – 2828	2000	10.0	4.0	6.2	62.0
2828 – 5656	4000	6.6	1.1	6.1	92.4
5656 – 11312	8000	15.4	1.1	3.6	24.3
11312 – 22624	16000	22.1	5.9	10.0	45.2

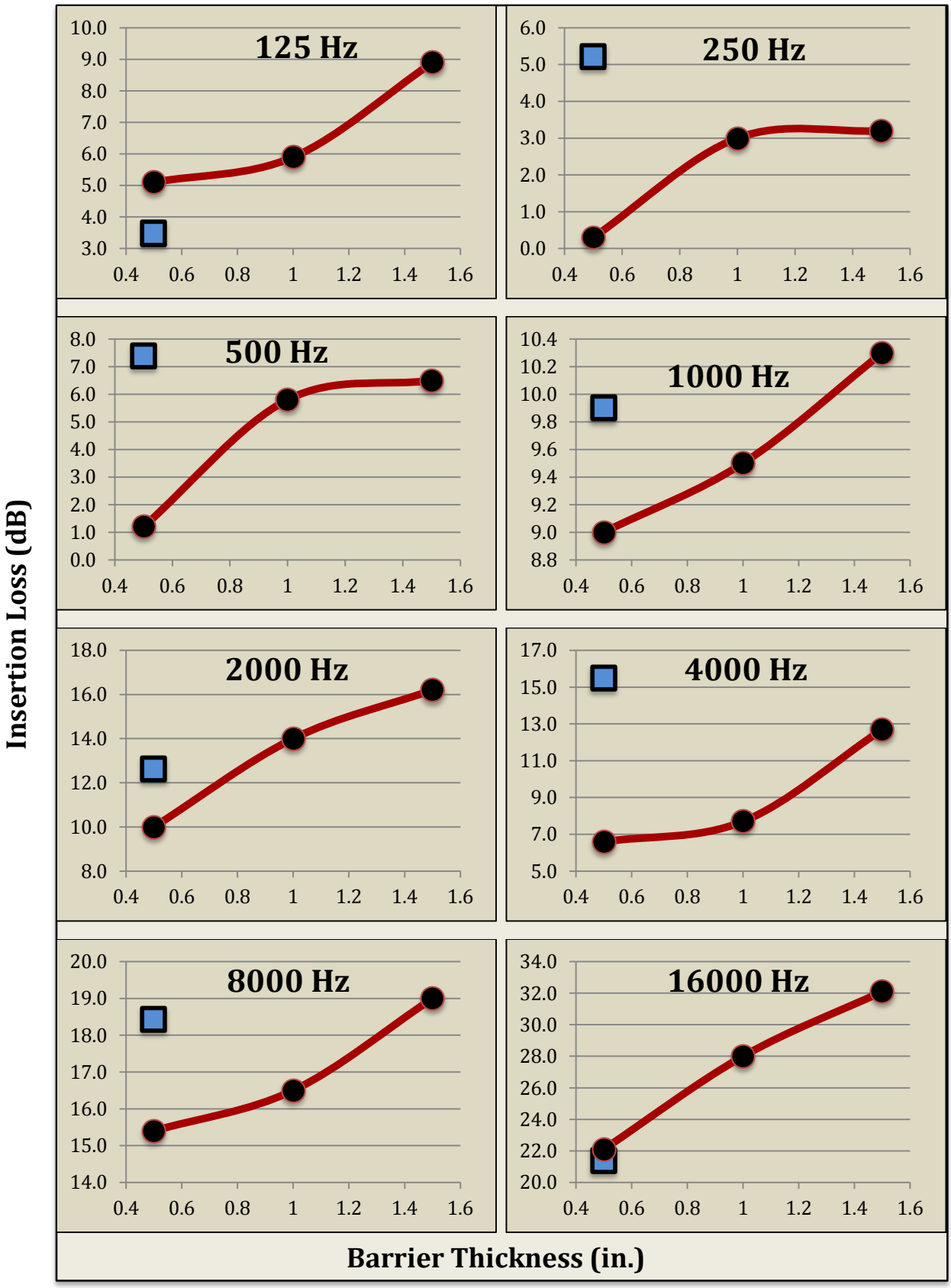

Figure 5.8. Measured (solid line) and theoretical (squares) IL for varying barrier thickness

It can be observed from Table 5.1 that improvement in TL by increasing barrier thickness leads to significant improvement in overall noise attenuation. The percentage increase in IL could seem to be remarkable for some of the source frequencies, however, percentage increment should be accepted with caution since the decibel scale is logarithmic and high percentage improvement does not necessarily correlate to significant improvement in noise attenuation. It is therefore more advisable to note the actual TL improvements in decibels. The incremental increase in TL is plotted in Figure 5.9 for the 1.0 in. and 1.5 in. barrier setups. Although the TL for the 0.5 in. barrier case was not zero, it is the baseline for incremental TL and was considered to be zero for the purpose of visualizing this incremental data. The experimental setups have TL improvements ranging from 0.5 dB to 5.9 dB for the 1.0 in. barrier and 1.3 dB to 10 dB for the 1.5 in. barrier. These values show that TL is playing a vital role in the noise attenuation of finite barriers along with diffraction.

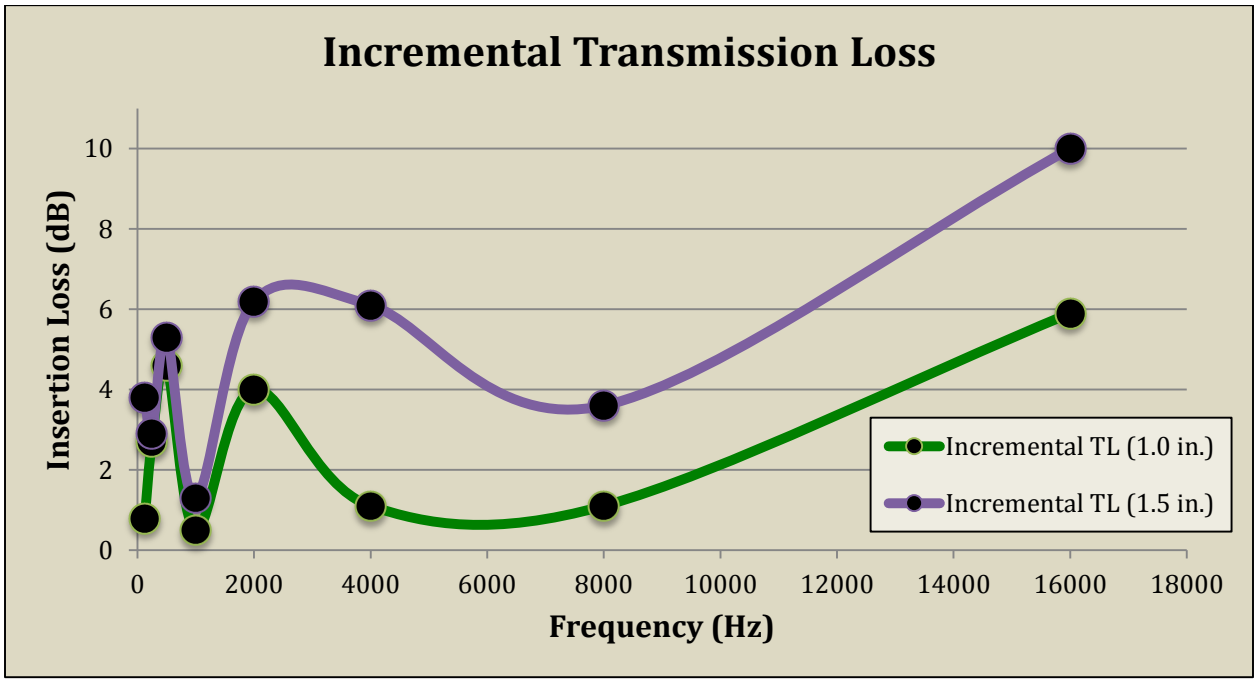

Figure 5.9. Incremental TL for the 1.0 in. and 1.5 in. barrier setups

5.6 Health, Safety, and Design Considerations

High decibel enhancements in TL should be of particular importance in the process of barrier design. An improvement of 10 dB could be extremely crucial depending on the barrier application. For example, according to OSHA regulations, sound levels that are above 90 dBA[7] could be hazardous to human health and safety [18]. There are strict exposure limits for noise levels that exceed this value. For example, the maximum occupational exposure limit for a sound level of 100 dBA is 2 hours. A reduction in sound level exposure from 100 dBA to 95 dBA or 90 dBA increases the maximum exposure time from 2 hours to 4 hours or 8 hours respectively[8]. Such a significant increase in exposure time could be of high importance in manufacturing plants or noisy office environments. It would not only improve employee safety but would also allow them and their employers to have more effective work plans with longer exposure times. It is also important to consider the financial aspect of such improvements because the incremental cost of obtaining thicker barriers for materials like plywood is generally low. If the areal dimensions of the barrier are constrained, it could be more cost-effective to improve TL by using thicker barriers rather than considering more expensive absorptive treatments to improve noise attenuation.

Improving barrier design should also correspond to reducing the wastefulness of material. Although higher barrier thicknesses lead to better noise attenuation, it is usually important not to optimize TL in every situation because optimized solutions are generally associated with higher costs. The best designs offer improvements but are also cost-effective and the solutions they provide tend to barely meet the performance requirements. For example, a 0.25 in. barrier could

[7] The use of dBA signifies the use of the A-weighted frequency scale, which applies established weighting corrections for the measurement of sound levels at each frequency [2]

[8] The maximum exposure time doubles for every 5 dBA reduction in continuous sound levels [18]

be sufficient to meet noise attenuation requirements in a particular situation even though the TL is extremely low. In such cases, it would be highly irresponsible to waste material and increase costs. The numerous evidences of the interdependence of diffraction theory and TL in the overall noise attenuation underline the importance of understating this relationship in order to deliver competitive noise control solutions.

CHAPTER VI: LIMITATIONS

The Moreland and Musa diffraction model for predicting noise attenuation exclusively applies to thin barriers. The model assumes that diffraction occurs at a single edge for each travel path when sound waves bend around a barrier. Beyond a certain barrier thickness, the bending sound waves depart from single edge diffraction behavior and diffraction occurs at two edges of the barrier. The diagram in Figure 6.1 shows double edge diffraction for thick barriers. Although the theory discussed in Chapter 3 is for thin barriers, the underlying principle of the theory is the concept of path difference. This path difference concept could also be applied to thicker barriers by making appropriate modifications. The basic principle of such a modification in path difference measurement is also shown in Figure 6.1. Specifically designed IL experiments would be required to verify the significance of this theoretical concept.

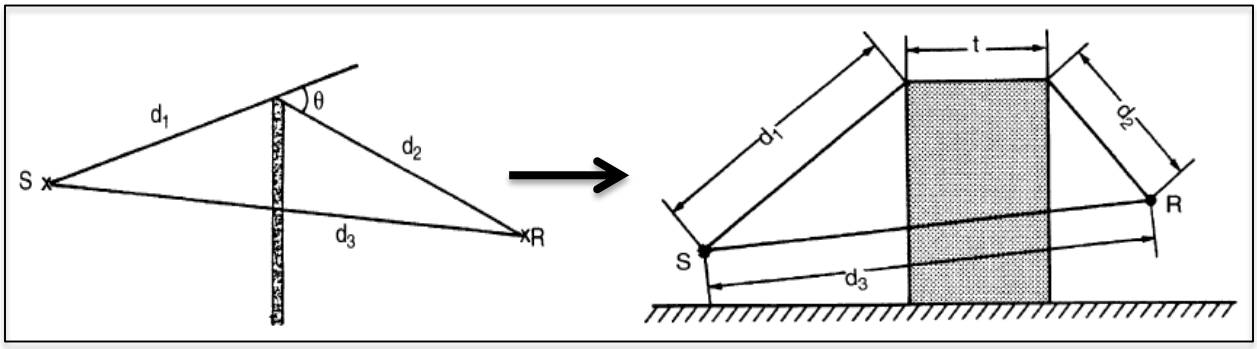

Figure 6.1. Thin barrier single edge diffraction and thick barrier double edge diffraction [8]

Common examples of thick barriers are berms or buildings. For sound frequencies of interest to the human ear, barrier thicknesses (t) greater than 10 ft. fall under the category of

thick barriers. For barrier thicknesses less than 10 ft., a barrier is considered to be thick if the source sound has a wavelength less than t/5 [8].

Modifying barrier material and thickness to improve the TL can be a useful strategy but it could prove to be wasteful if the design is over optimized. Improving TL implies that the transmission of sound through the barrier approaches zero, however, as the TL reaches this limiting condition, an increase in barrier thickness would prove to be wasteful and would not offer any significant noise attenuation benefits.

CHAPTER VII: CONCLUSIONS AND FUTURE WORK

7.1 Conclusions

The experimental methods used in this study are effective in isolating transmission loss from diffraction based noise attenuation. The experimental observations showed that TL was a significant part of the overall IL provided by the barrier. The theoretical predictions were generally found to be larger than the experimental IL for the thin barrier. However, as the barrier thickness increased, the experimental values were found to be increasing as they converged upon theoretical predictions. This provides strong evidence that the Moreland and Musa theory does not consider TL as a factor in IL predictions. The predictions do, however, estimate the diffraction based noise attenuation with considerable accuracy. This conclusion is based on the convergence of experimental IL values to the theoretical ones for increasing barrier thickness because thicker barriers imply a reduction in the transmission of sound waves through the barrier.

Further evidence of the influence of TL is observed at low frequency measurements. The fluctuations observed in noise attenuation agree with the effect of panel resonances for TL through materials. The drop in the experimental IL values observed at 4000 Hz also provides a strong indication of the impact of TL. According to TL theory, a considerable drop in TL is experienced at a high frequency, which has a negative influence on noise attenuation. This behavior was consistently observed in all the experimental setups. These observations show a

continuous interplay between diffraction and TL in the performance of finite barriers and encourage adequate attention from acoustical engineers while designing noise control solutions using finite barriers.

Understanding TL could prove valuable in achieving improved noise attenuation solutions, but it is also important to understand its limitations. While increasing the barrier thickness can improve the overall IL, it is not an indefinite increase. As the transmission of sound through the barrier approaches zero, any increase in barrier thickness would prove to be wasteful and expensive without any performance gains. It is therefore advisable to carefully acknowledge the observations made in this study and use these concepts in designing noise control solutions.

This study highly recommends an investigation of the dominant source frequency responsible for noise problems while designing finite barrier solutions. The frequency dependent nature of diffraction and TL makes it an essential factor of the design process. Understanding the problematic frequencies would help the designer choose barrier material and thicknesses so that the critical frequency of the barrier does not coincide with the dominant source frequency. If the areal dimensions of the barrier are constrained due to the geometrical or architectural setup of the noise area, an acoustical engineer can use TL concepts to achieve the required noise attenuation by choosing the appropriate material and thickness. While it was observed that the TL also affected barrier performance at lower frequencies through panel resonances, it is important to note that the IL at these frequencies is considerably low. The cost-effectiveness of increasing barrier thickness for improving low frequency IL should be investigated cautiously. In certain situations, it may be more cost effective to use absorptive barriers to reduce the transmission of sound rather than invest in increased barrier thickness.

There are numerous interacting factors within the concepts of TL and diffraction, which depend on material, thickness, source frequency, etc. The interactions observed in this study show that using this knowledge could go a long way in achieving solutions to modern noise control problems. If designed appropriately, they could double or triple the allowed exposure times in manufacturing environments and lead to tremendous health and cost benefits.

7.2 Future Work

This study is limited to investigating the impact of TL for a fixed distance from the source and the barrier. This setup, which included constant path differences, was necessary to take advantage of the Fresnel Number concept. However, it is a well-established fact that the proximity of the barrier to the source has a direct impact on diffraction based noise attenuation. Therefore, studying the impact of TL as the proximity between the barrier and the source is varied could prove to be extremely valuable.

The experiments in this study were exclusively conducted on a plywood barrier. It was chosen since it is standard construction material that is fairly inexpensive and commonly used in barrier structures. The same experiments could be repeated using alternative barrier materials. Comparing the data obtained from different materials could provide some useful insight in understanding how TL interacts with diffraction in affecting the overall barrier performance.

Performing experiments using absorptive barrier material could also be an interesting area of investigation. Absorptive treatment on the source side of the barrier would theoretically render the effects of TL to be negligible in non-reverberant spaces, and leave the diffraction effects to dominate the overall barrier performance. However, it would be very useful to compare this theoretical concept to experimental observations.

This study provides a strong evidence of the impact of TL on finite barrier performance. However, a quantitative analysis of the impact of TL was not in the scope of this study. A broad quantitative relationship connecting the TL effect based on surface density and the diffraction effect based on areal dimensions of the barrier, and the proximity of the source to the barrier would be invaluable for acoustical engineers. It would allow them to comprehensively investigate material and thickness options to provide effective and inexpensive finite barrier solutions to noise control problems in the industrial and residential sphere.

LIST OF REFERENCES

1. Occupational Safety and Health Administration of the United States of America. OSHA. 20 February 2015 <https://www.osha.gov/about.html>.

2. Bell, Lewis H. and Douglas H. Bell. Industrial Noise Control. Ed. L. L. Faulkner. 2nd Edition. New York: Marcel Dekker, INC., 1994.

3. Maekawa, Z. "Noise Reduction by Screens." Applied Acoustics 1.3 (1968): 157-173.

4. Moreland, J. B. and R. S. Musa. "The Performance of Acoustic Barriers." Proceedings of Inter-Noise72. Washington D.C., 1972. 95-104.

5. Iyer, Neel. "Evaluation of Methods for Predicting Acoustical Insertion Loss of Barriers in Enclosed Spaces." Diss. Rose-Hulman Institute of Technology, 2013.

6. Upasani, Ashwin A. and Zhao Li. *Project Report: Study Insertion Loss due to Finite Barriers.* 18 Nov. 2013. TS. Rose-Hulman Institute of Technology, Terre Haute, IN. USA.

7. Barboza, Tony. "Long beach hopes mulch wall will make Hudson Park and healthier place." Los Angeles Times 6 Aug. 2013 < http://articles.latimes.com/2013/aug/06/local/la-me-mulch-wall-20130807>

8. International Institute of Noise Engineering. Technical Assessment of the Effectiveness of Noise Walls. 15 Nov. 1998. 27 Feb. 2015. <http://i-ince.org/files/publications/iince991.pdf>

9. Kurze., U. J. and G. S. Anderson. "Sound Attenuation by Barriers." Applied Acoustics 4.1 (1971): 35-53.

10. United States. Federal Highway Administration. *Highway Traffic Noise. Noise Barrier Design Handbook.* Washington: Department of Transportation, Federal Highway Administration, 2011. Web. 17 Feb 2015. <http://www.fhwa.dot.gov/environment/noise/noise_barriers/design_construction/design/design03.cfm>

11. Beranek, Leo L. and István L. Ver. Noise and Vibration Control. Ed. Leo L. Beranek and István L. Ver. 2nd Edition. Hoboken: John Wiley and Sons, Inc., 2006.

12. Soedel, Werner. Vibrations of Shells and Plates. 3rd Edition. New York: Marcel Dekker, Inc., 2004.

13. Purcell, W. E. "Materials for Noise and Vibration Control." Sound and Vibration 10 (1977): 20.

14. Gremore, Adam. "The Development and Evaluation of an Improved Method for Measuring Transmission Loss through Partitions." Diss. Rose-Hulman Institute of Technology, 2006.

15. Thornhill, Ted. "We all crave it, but can you stand the silence? The longest anyone can bear the Earth's quietest place is 45 minutes." The Daily Mail 3 Apr. 2012 < http://www.dailymail.co.uk/sciencetech/article-2124581/The-worlds-quietest-place-chamber-Orfield-Laboratories.html>

16. Beranek, Leo L. and Harvey P. Sleeper. "The Design and Construction of Anechoic Sound Chambers." The Journal of the Acoustical Society of America 18.1 (1946): 140-150.

17. Pompei, Anna, M. A. Sumbatyan and N. F. Todorov. "Computer Models in Room Acoustics: The Ray Tracing Method and the Auralization Algorithms." Acoustical Physics 55.6 (2009): 821-831.

18. Occupational Health and Safety Administration. "Occupational Noise Exposure." *U.S. Department of Labor, Occupational Safety and Health Administration.* Web. 22 Feb. 2015. <https://www.osha.gov/pls/oshaweb/owadisp.show_document?p_table=STANDARDS&p_id=9735#1910.95%28b%29%282%29>

APPENDICES

Appendix A

Appendix A shows the ambient SPL measured in the anechoic chamber before barrier insertion. Table A.1 shows the ambient SPL for the center frequencies of the measured octave bands. Additionally, Table A.2 also shows the ambient SPL for the center frequencies of one-third octave bands between 2000 Hz and 8000 Hz.

Table A.1. Ambient SPL measurements for octave band center frequencies

Octave Band (Hz)	Frequency (Hz)	Ambient Sound (dB)
88-177	125	16.2
177-354	250	13.5
354-707	500	10.6
707-1414	1000	5.6
1414-2828	2000	1.2
2828-5656	4000	0.4
5656-11312	8000	2.0
11312-22624	16000	2.6

Table A.2. Ambient SPL measurements for one-third octave band center frequencies

1/3rd Octave Band (Hz)	Frequency (Hz)	Ambient Sound (dB)
1778-2239	2000	1.2
2239-2828	2500	3.7
2828-3548	3150	1.9
3548-4467	4000	0.4
4467-5656	5000	2.3
5656-7079	6300	0.8
7079-8913	8000	2.0

Appendix B

Appendix B shows the SPL measurements that were documented for all the experimental setups. Table B.1 shows how the SPL varied during barrier insertion of increasing thicknesses. These SPL values were used to calculate the IL for each experimental setup and this information is displayed in Table B.2.

Table B.1. SPL measurements before and after barrier insertion for each experimental setup

Octave Band (Hz)	Frequency (Hz)	SPL Before Insertion (dB)	SPL [0.5 in. barrier] (dB)	SPL [1.0 in. barrier] (dB)	SPL [1.5 in. barrier] (dB)
88-177	125	62.1	57.0	56.2	53.2
177-354	250	65.2	64.9	62.2	62.0
354-707	500	49.6	48.4	43.8	43.1
707-1414	1000	56.0	47.0	46.5	45.7
1414-2828	2000	49.3	39.3	35.3	33.1
2828-5656	4000	54.6	48.0	46.9	41.9
5656-11312	8000	53.3	37.9	36.8	34.3
11312-22624	16000	54.7	32.6	26.7	22.6
1778-2239	2000	49.3	39.3	35.3	33.1
2239-2828	2500	56.8	42.4	40.2	39.5
2828-3548	3150	55.6	34.2	32.3	30.6
3548-4467	4000	54.6	46.0	44.9	39.9
4467-5656	5000	59.5	45.0	42.0	39.1
5656-7079	6300	60.7	44.9	44.9	40.3
7079-8913	8000	53.3	37.9	36.8	34.3

Table B.2. Experimental IL values for each setup at the octave band center-frequencies

Octave Band (Hz)	Frequency (Hz)	IL [0.5 in barrier] (dB)	IL [1.0 in barrier] (dB)	IL [1.5 in barrier] (dB)
88-177	125	5.1	5.9	8.9
177-354	250	0.3	3.0	3.2
354-707	500	1.2	5.8	6.5
707-1414	1000	9.0	9.5	10.3
1414-2828	2000	10.0	14.0	16.2
2828-5656	4000	6.6	7.7	12.7
5656-11312	8000	15.4	16.5	19.0
11312-22624	16000	22.1	28.0	32.1
1778-2239	2000	10.0	14.0	16.2
2239-2828	2500	14.4	16.6	17.3
2828-3548	3150	21.4	23.3	25.0
3548-4467	4000	8.6	9.7	14.7
4467-5656	5000	14.5	17.5	20.4
5656-7079	6300	15.8	15.8	20.4
7079-8913	8000	15.4	16.5	19.0

Appendix C

Appendix C shows the experimental setup in the anechoic chamber after barrier insertion.

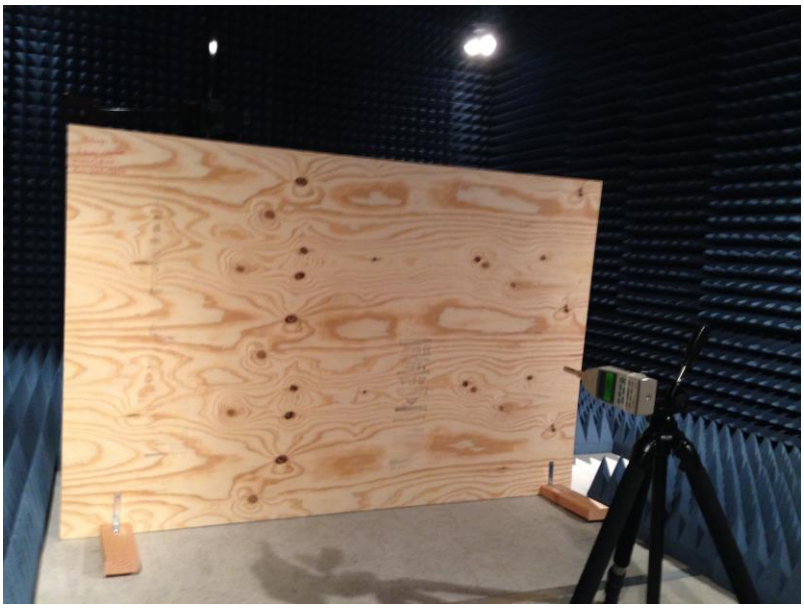

Figure C.1. The receiver side of the anechoic chamber after barrier insertion

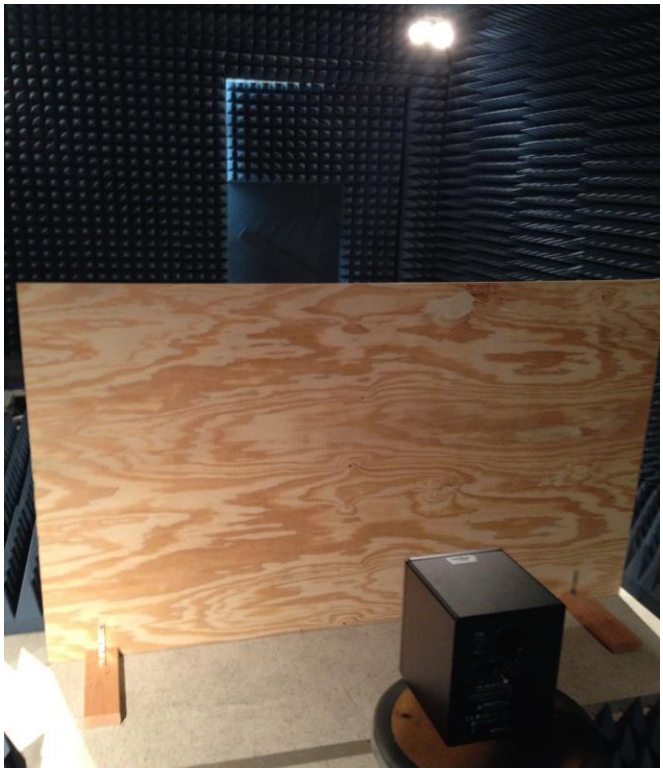

Figure C.2. The source side of the anechoic chamber after barrier insertion

Appendix D

Appendix D shows the detailed theoretical calculations of insertion loss, which are based on equation 3.12. The Fresnel Numbers for each diffraction path for all the measured frequencies are shown in Table D.1. These Fresnel numbers were then used to get the theoretical IL values that are also shown in the table below.

Table D.1. Fresnel numbers and theoretical IL values for the measured frequencies

Octave Band (Hz)	Frequency (Hz)	Wavelength (m)	N1	N2	N3	IL [theoretical] (dB)
88-177	125	2.64	0.2188	0.2691	0.9391	3.5
177-354	250	1.32	0.4377	0.5381	1.8781	5.2
354-707	500	0.66	0.8753	1.0762	3.7562	7.4
707-1414	1000	0.33	1.7507	2.1525	7.5125	9.9
1414-2828	2000	0.17	3.5014	4.3049	15.0250	12.6
2828-5656	4000	0.08	7.0028	8.6099	30.0500	15.5
5656-11312	8000	0.04	14.0055	17.2198	60.0999	18.4
11312-22624	16000	0.02	28.0111	34.4396	120.1998	21.4
1778-2239	2000	0.17	3.5014	4.3049	15.0250	12.6
2239-2828	2500	0.13	4.3767	5.3812	18.7812	13.5
2828-3548	3150	0.10	5.5147	6.7803	23.6643	14.5
3548-4467	4000	0.08	7.0028	8.6099	30.0500	15.5
4467-5656	5000	0.07	8.7535	10.7624	37.5624	16.4
5656-7079	6300	0.05	11.0294	13.5606	47.3287	17.4
7079-8913	8000	0.04	14.0055	17.2198	60.0999	18.4